

# Exact Sampling of Jump-Diffusions

Kay Giesecke\* and Dmitry Smelov†

August 20, 2010

This draft: May 8, 2012‡

*Operations Research*, forthcoming

## Abstract

Jump-diffusion processes are ubiquitous in finance and economics. They arise as models of security, energy and commodity prices, exchange and interest rates, and default timing. This paper develops a method for the exact simulation of a skeleton, a hitting time and other functionals of a one-dimensional jump-diffusion with state-dependent drift, volatility, jump intensity and jump size. The method requires the drift function to be  $C^1$ , the volatility function to be  $C^2$ , and the jump intensity function to be locally bounded. No further structure is imposed on these functions. The method leads to unbiased simulation estimators of security prices, transition densities, hitting probabilities, and other quantities. Numerical results illustrate its features.

---

\*Department of Management Science & Engineering, Stanford University, Stanford, CA 94305-4026, USA, Phone (650) 723 9265, Fax (650) 723 1614, email: [giesecke@stanford.edu](mailto:giesecke@stanford.edu), web: [www.stanford.edu/~giesecke](http://www.stanford.edu/~giesecke).

†Department of Management Science & Engineering, Stanford University, Stanford, CA 94305-4026, USA, email: [dsmelov@stanford.edu](mailto:dsmelov@stanford.edu).

‡This paper was presented at the Sixth World Congress of the Bachelier Finance Society in Toronto and the 17th International Conference on Computing in Economics and Finance in San Francisco. We thank conference participants for comments. We are grateful to Nan Chen, Mike Giles, Peter Glynn, Eckhard Platen, Bruno Remillard, Gerald Teng and two anonymous referees and an associate editor for insightful comments.

# 1 Introduction

Jump-diffusions are widely used as models for the time evolution of prices and rates in equity, fixed income, commodity, foreign exchange, energy and other markets. They also serve as models of default timing in portfolios of credit-sensitive assets such as loans and corporate bonds. Monte Carlo simulation is an important tool to address the pricing, risk management and inference problems arising in this context. Relative to alternative numerical approaches, simulation has the widest scope. It requires few restrictions on the coefficients of the jump-diffusion and the functional to be evaluated.

The standard approach to simulating a jump-diffusion with state-dependent drift, volatility, jump intensity, and jump size is to approximate it on a discrete-time grid; see Platen & Bruti-Liberati (2010) for a comprehensive analysis. The diffusion component is treated with an Euler or higher order discretization scheme. If the jump intensity is bounded, the jump times can be sampled exactly using a thinning scheme. In the general case, the jump times are approximated using a time-scaling scheme. While often easy to implement, the approximations introduce bias into the simulation estimator. Since the magnitude of the bias is usually unknown, it is difficult to obtain valid confidence intervals. Many time steps may be required to reduce the bias to an acceptable level, and even more computational effort is needed to verify that the bias is small enough. Moreover, the optimal allocation of the computational budget between the number of time steps and the number of trials is difficult to specify in advance.

This paper develops a method for the *exact* sampling of a one-dimensional jump-diffusion with state-dependent drift, volatility, jump intensity, and jump size. The algorithm requires the drift function to be  $C^1$ , the volatility function to be  $C^2$ , and the jump intensity function to be locally bounded. No further structure is imposed on these functions. The method generalizes an acceptance/rejection scheme developed for certain one-dimensional diffusions  $X$  by Beskos & Roberts (2005) and its extension to a wider class of diffusions developed by Chen (2009). The basic idea is to sample a path of a standard Brownian motion  $W$ , and to accept that path as one of  $X$  with a probability proportional to the Radon-Nikodym derivative between the law of  $X$  and the law of  $W$ . The generation of the acceptance indicator is based on a thinning mechanism exploiting the observation that the Radon-Nikodym derivative is analogous to the conditional probability that a doubly-stochastic Poisson process does not jump during some interval. We extend this approach to address the presence of jumps in  $X$  that arrive at a state-dependent intensity and have a state-dependent magnitude. At the same time, we relax some of the conditions on the drift and volatility functions assumed in the aforementioned articles, thereby widening the scope of the acceptance/rejection scheme even for diffusions. Moreover, we enlarge the class of expectations that can be treated exactly. These include expectations of functionals depending on a skeleton of  $X$ , the complete path of the jump component, a hitting time, and the value of  $X$  at the hitting time, as well as the expectation of the exponential of the time-integral of  $X$ .

The exact jump-diffusion method eliminates the need to quantify and reduce discretization bias. It leads to unbiased simulation estimators of security prices, transition densities, hitting probabilities and other quantities. Numerical experiments illustrate the performance of the method for the valuation of European, discretely monitored Asian and barrier options under the jump-to-default extended CEV model of Carr & Linetsky (2006), and for the valuation of bonds under an affine jump-diffusion model of the short rate. The exact method achieves the optimal square-root convergence, and often attains a specified level of accuracy faster than a discretization scheme.

The exact method developed in this paper has a wider scope than alternative methods for the exact simulation of jump-diffusions. Unlike other schemes, our method applies to standard parametric models with unbounded and potentially discontinuous jump intensity, including the affine jump-diffusions of Duffie, Pan & Singleton (2000) and the non-linear jump-diffusions of Andersen & Buffum (2003), Ayache, Forsyth & Vetzal (2003), Carr & Linetsky (2006), Carr & Madan (2010), Davis & Lischka (2002), Linetsky (2006), Mendoza, Carr & Linetsky (2010), and others. Our method allows for the exact treatment of the non-parametric, state-dependent jump-diffusion models in the empirical finance literature, such as the short rate model of Johannes (2004). It also facilitates the simulation based analysis of the properties of the corresponding estimators as in Ait-Sahalia, Fan & Peng (2009), Bandi & Nguyen (2003) and others, and simulation based inference for state-dependent jump-diffusion models. The feasibility of exact sampling eliminates the need to analyze the implications of discretization errors for the inference process. Moreover, our method facilitates the exact treatment of the jump-diffusion default intensity models proposed in a substantial literature on single-name and portfolio credit risk, which includes Arnsdorf & Halperin (2008), Ding, Giesecke & Tomezek (2009), Duffie & Singleton (1999), Madan & Unal (1998) and many others. It also facilitates the exact treatment of first-passage credit models, in which the firm value follows a jump-diffusion and default occurs when that value hits a barrier, as in Zhou (2001).

The existing jump-diffusion algorithms require additional restrictions on the coefficient or jump intensity functions. If the intensity is not state-dependent as in the models of Merton (1976), Kou (2002) and Kou & Wang (2004), then the jumps arrive according to a Poisson process. In this case the jump times can be generated exactly, independently of the diffusion component. The schemes of Beskos & Roberts (2005) or Chen (2009) provide exact samples of a skeleton of the diffusion component between the jump times, even if the diffusion has a state-dependent drift or volatility. Broadie & Kaya (2006) develop an alternative exact scheme for the two-dimensional Heston model with constant intensity jumps in volatility and price. Ruf & Scherer (2011) consider the exact sampling of the hitting time of a constant intensity jump-diffusion.

If the jump intensity is state-dependent, then the jump times cannot be generated independently of the diffusion component. Casella & Roberts (2011) treat the case of a uniformly bounded jump intensity. They combine the diffusion scheme of Beskos & Roberts (2005) with the state-dependent thinning scheme of Glasserman & Merener (2003)

for the jump times. Our approach extends the localization approach of Chen (2009), and does not require the jump intensity to be bounded. The jump-diffusion is decomposed into bounded segments between the jump times and an acceptance/rejection mechanism is sequentially applied to each of these segments.

Giesecke, Kakavand & Mousavi (2010) develop an exact scheme for a point process with a general state-dependent intensity. If the intensity is driven by a jump-diffusion whose jump times are those of the point process, then this scheme also provides exact samples of a skeleton of the jump-diffusion. However, this scheme imposes some structure on the coefficient and jump intensity functions. The method proposed here does not require such structure, but may be slower than the method of Giesecke et al. (2010) for certain functionals and parameter configurations.

The rest of this paper is organized as follows. Section 2 introduces the jump-diffusion, states the assumptions, and performs a transformation. Section 3 develops the exact scheme, Section 4 discusses extensions and Section 5 explains the implementation. Sections 6 and 7 provide numerical results. Section 8 concludes. An appendix details a proof.

## 2 Preliminaries

### 2.1 Jump-diffusion process

Fix a complete probability space  $(\Omega, \mathcal{F}, \mathbb{P})$  and a right-continuous and complete information filtration  $\mathbb{F} = (\mathcal{F}_t)_{t \geq 0}$ . Consider a process  $X$  in a state space  $D_X$ , a connected subset of  $\mathbb{R}$ . Up to the hitting time of the boundary of  $D_X$ ,  $X$  is the unique weak solution to the stochastic differential equation (SDE)

$$dX_t = \mu(X_t)dt + \sigma(X_t)dW_t + dJ_t \quad (1)$$

where the initial value  $X_0 \in I_X = \text{Int } D_X$ , the drift function  $\mu : I_X \rightarrow \mathbb{R}$ , the volatility function  $\sigma : I_X \rightarrow (0, \infty)$ ,  $W$  is a standard Brownian motion and  $J$  is a jump process

$$J_t = \sum_{n=1}^{N_t} \Delta(X_{T_n-}, Z_n). \quad (2)$$

The process  $N$  is a non-explosive counting process with event times  $(T_n)_{n \geq 1}$  and intensity  $\lambda_t = \Lambda(X_{t-})$ , where  $\Lambda : I_X \rightarrow [0, \infty)$ . Further,  $(Z_n)_{n \geq 1}$  is a sequence of mark variables valued in  $E \subseteq \mathbb{R}$ . A variable  $Z_n$  encodes additional information revealed at a jump time  $T_n$ , and is drawn from a fixed distribution  $\Pi$ . The function  $\Delta : I_X \times E \rightarrow \mathbb{R}$  specifies the jump magnitude at  $T_n$  as a function of  $Z_n$  and the state just before  $T_n$ .

We do not impose a specific structure on  $(\mu, \sigma, \Lambda, \Delta, \Pi)$ . In order for the SDE (1) to have a unique weak solution up to the hitting time of the boundary of  $D_X$ , there are technical restrictions on  $(\mu, \sigma, \Lambda, \Delta, \Pi)$ . See, e.g., Ikeda & Watanabe (1989).

The jump-diffusion process (1) permits the volatility coefficient  $\sigma(X)$  to be a function of the state; it constitutes a “local” volatility model with jumps. The jump process (2) is self-affecting, because the jump intensity  $\lambda$  is a function of the state and therefore depends on the timing and size of past jumps. Thus, a jump has an impact on the current and future jump frequency. Moreover, there is an intricate dependence structure between the state, the jump frequency, and the jump magnitude. The jump magnitude depends on the state prior to the jump and also influences the future evolution of the state, which in turn has an impact on the jump intensity.

The formulation (1)–(2) can be extended to time-dependent jump intensity and jump size functions, and to include the dependency of these functions on  $(J_{t-}, N_{t-})$ . The time-dependency can be useful in the context of model calibration. The jump-dependency can be used to control the jump behavior as a function of the jump state. These generalizations merely involve notational changes.

## 2.2 Objective

Our primary objective is to generate exact samples of

$$((X_t)_{t \in S}, (N_t, J_t)_{t \leq T}, \xi, X_\xi) \quad (3)$$

where  $T > 0$  is a fixed horizon,  $S$  is a finite set of fixed times  $t \in [0, T]$ ,

$$\xi = \inf\{t \leq T : X_t \leq \ell\} \quad (4)$$

is the hitting time of  $X$  to a level  $\ell < X_0$ , and  $X_\xi$  is the value at the hitting time. Exact samples of (3) generate an *unbiased* Monte Carlo estimator of the expectation  $V = \mathbb{E}[v((X_t)_{t \in S}, (N_t, J_t)_{t \leq T}, \xi, X_\xi)]$  for a suitable function  $v$ . In statistical applications, if  $X$  models the price of an underlying asset or rate under the empirical measure  $\mathbb{P}$ ,  $V$  could represent the distribution or some statistic of  $(X_t)_{t \in S}$ . In derivatives pricing applications,  $\mathbb{P}$  is a risk-neutral measure and  $V$  could represent the price of a derivative with payoff depending on (3). Examples include European, discretely monitored Asian, and barrier options. In first-passage structural models of default,  $X$  represents the value of a firm and  $V$  could represent the probability of default or the values of corporate securities such as equity or bonds. In a reduced-form setting,  $N$  counts defaults in a portfolio of firms, the jump sizes  $\Delta$  model position losses, and  $J$  represents the portfolio loss. Here  $V$  could represent the value of a credit derivative referenced on the portfolio. The ability to treat a functional  $v$  depending on the path  $\{N_t, J_t : 0 \leq t \leq T\}$  is convenient in this context, because the discounted cash flows of standard portfolio derivatives can be represented as Stieltjes integrals against that path. See Errais, Giesecke & Goldberg (2010) for examples. Aside from  $V$ , we are also interested in the expectation  $\mathbb{E}[\exp(-\int_0^T X_s ds)u((X_t)_{t \in S}, (N_t, J_t)_{t \leq T})]$  for suitable  $u$ , which could represent the value of a fixed-income security such as a bond when  $X$  models the short-term rate of interest.

## 2.3 Assumptions

Our method for generating exact samples of (3) requires the following assumptions. These assumptions define the scope of the method.

**Assumption 2.1.** *On  $I_X = \text{Int} D_X$ ,  $\mu$  is continuously differentiable,  $\sigma$  is twice continuously differentiable, and  $\Lambda$  is locally bounded.*

Many standard jump-diffusion models have smooth coefficient functions and a locally bounded intensity function. Examples include the affine jump-diffusions of Duffie et al. (2000), the non-linear jump-diffusions with power intensity of Carr & Linetsky (2006), Carr & Madan (2010), Linetsky (2006) and Mendoza et al. (2010), and the pure jump models of Arnsdorf & Halperin (2008), Ding et al. (2009), Duffie & Singleton (1999), Madan & Unal (1998) and many others. In these formulations, the jump intensity is locally bounded but not uniformly bounded.

**Assumption 2.2.** *The boundary of  $D_X$  is either unattainable or attainable only through a jump. In the latter case the boundary is absorbing.*

This assumption primarily addresses the non-linear jump-diffusion processes of Carr & Linetsky (2006), Carr & Madan (2010), Linetsky (2006), Mendoza et al. (2010) and others. In these models,  $X$  is strictly positive until its first jump, at which time it drops to 0 and does not recover. Here  $D_X = [0, \infty)$ , where 0 is an absorbing boundary that can be attained only through a jump.

## 2.4 Unit-volatility jump-diffusion

It is convenient to transform  $X$  into a jump-diffusion with unit volatility. Consider the Lamperti transform

$$F(x) = \int_{X_0}^x \frac{1}{\sigma(u)} du, \quad x \in I_X, \quad (5)$$

which is monotone and finite for all  $x \in I_X$ . The inverse of  $F$  exists on  $I_X$  and is denoted by  $F^{-1}$ . Consider the transformed variable  $Y_t = F(X_t)$ . If the boundary  $\partial D_X = \{\underline{x}\} \cup \{\bar{x}\}$  of  $D_X$  is unattainable, then  $Y$  does not attain the boundary  $\partial D_Y = \{\underline{y}\} \cup \{\bar{y}\}$  of its domain  $D_Y \subseteq \mathbb{R}$  either. However, if  $X$  can reach  $\partial D_X$  through a jump, we extend the transform (5) to the boundary:

$$F(\underline{x}) = \underline{y}, \quad F(\bar{x}) = \bar{y}. \quad (6)$$

By Itô's formula,  $Y_t = F(X_t)$  solves the SDE

$$dY_t = \mu_Y(Y_t)dt + dW_t + dJ_t^Y \quad (7)$$

up to the hitting time of  $\partial D_Y$ . Here,  $Y_0 = F(X_0) = 0$  and the drift function

$$\mu_Y(y) = \frac{\mu(F^{-1}(y))}{\sigma(F^{-1}(y))} - \frac{1}{2}\sigma'(F^{-1}(y)) \quad (8)$$

is continuous on  $\text{Int } D_Y$ . The jump process  $J^Y$  in the SDE (7) has the same jump times as the jump process  $J$  in the SDE (1); only the jump sizes are different. We have

$$J_t^Y = \sum_{n=1}^{N_t} \Delta_Y(Y_{T_n-}, Z_n) \quad (9)$$

where, for  $y \in \text{Int } D_Y$  and  $z \in E$ , the jump size function

$$\Delta_Y(y, z) = F(F^{-1}(y) + \Delta(F^{-1}(y), z)) - y. \quad (10)$$

If  $X$  can reach  $\partial D_X$  through a jump, then  $Y$  can reach  $\partial D_Y$  through a jump. The boundary of  $X$  is absorbing, and so is the boundary of  $Y$ .

We illustrate with an example.

**Example 2.3.** For constants  $\mu, \Lambda \geq 0$  and  $\sigma, X_0, c > 0$ , consider the specification

$$\mu(x) = \mu x, \quad \sigma(x) = \sigma x, \quad \Lambda(x) = \Lambda x, \quad \Delta(x, z) = x(z - 1) \wedge c. \quad (11)$$

If  $\Lambda = 0$ , then  $X$  is a geometric Brownian motion. If  $\Lambda > 0$ , then  $X$  jumps at an intensity proportional to  $X$ . The transform (5) takes the form

$$F(x) = \frac{1}{\sigma} \log \left( \frac{x}{X_0} \right), \quad x \in (0, \infty). \quad (12)$$

First, suppose the marks  $Z_n$  have support  $(0, \infty)$ . Then  $D_X = (0, \infty)$ . The boundary  $\partial D_X$  is unattainable, even if  $X$  jumps. The transform (12) takes  $D_X$  into  $D_Y = (-\infty, \infty)$ . The boundary  $\partial D_Y$  is unattainable. The process  $Y = F(X)$  has drift  $\mu_Y(y) = \mu/\sigma - \sigma/2$  and jump size  $\Delta_Y(y, z) = (\log z)/\sigma$ .

Next, suppose the marks  $Z_n = 0$ . Then  $D_X = [0, \infty)$ . The boundary  $\infty$  is unattainable. The boundary  $0$  is attainable only through a jump, which occurs at  $T_1$ . The transform (12) is extended to  $F(0) = -\infty$  and takes  $D_X$  into  $D_Y = [-\infty, \infty)$ . The boundary  $-\infty$  is attainable only through a jump; the jump size  $\Delta_Y(Y_{T_1-}, 0) = -\infty$ .

We focus on the problem of sampling the values and jump times of  $Y$  in the interval  $[0, T]$ . A sample of  $X_t$  can be recovered from a sample of  $Y_t$  by applying the inverse transformation  $F^{-1}(Y_t)$ . The jump times  $T_n$  of  $X$  are those of  $Y$ , and the associated jump magnitudes of  $X$  are given by  $\Delta(F^{-1}(Y_{T_n-}), Z_n)$ .

### 3 Exact method

This section describes an exact method for sampling the unit-volatility jump-diffusion  $Y$ . The method uses an acceptance/rejection mechanism, and we begin by discussing the basic idea and its application to sampling a diffusion.

#### 3.1 Acceptance/rejection

Suppose we want to sample from a density  $f(y)$ . If there is another density  $g(y)$  and a constant  $c > 0$  such that  $cf(y) \leq g(y)$ , then we can proceed as follows. We draw a sample  $Y$  from  $g$  and a Bernoulli variable  $I$  with success probability  $cf(Y)/g(Y)$ , and then accept  $Y$  as a sample from  $f$  if  $I = 1$ . This procedure is particularly advantageous whenever it is easier to sample from the proposal density  $g$  than from the target density  $f$ .

Beskos & Roberts (2005) use the acceptance/rejection method to draw an exact sample of  $Y_T$  when  $Y$  is a diffusion satisfying  $dY_t = \mu_Y(Y_t)dt + dW_t$ , i.e. when the jump intensity function  $\Lambda = 0$  on  $I_X$ . To explain the procedure, let

$$A(y) = \int_0^y \mu_Y(u)du \quad (13)$$

and assume that the drift  $\mu_Y$  of  $Y$  is such that  $C = \int_{\mathbb{R}} \exp(A(y) - y^2/(2T))dy$  is finite. Consider the proposal density  $g(y) = \exp(A(y) - y^2/(2T))/C$ . Assuming that  $\mu_Y$  satisfies Novikov's condition, Beskos & Roberts (2005) show that the density ratio

$$\frac{f_{Y_T}(y)}{g(y)} \propto \mathbb{E} \left[ \exp \left( - \int_0^T \phi(W_s)ds \right) \middle| W_T = y \right] =: H(y) \quad (14)$$

where

$$\phi(y) = \frac{1}{2}(\mu'_Y(y) + \mu_Y^2(y)). \quad (15)$$

For the acceptance test, one needs to generate a Bernoulli indicator  $I$  with success probability  $H(Y)$ , where  $Y$  is drawn from  $g$ . To this end, note that  $H(y) = \mathbb{P}(V_T = 0 \mid W_T = y)$  where  $V$  is a doubly-stochastic Poisson process with intensity  $\phi(W)$ , provided that  $\phi \geq 0$ . Thus, the required indicator can be generated by sampling the jump times of  $V$  during  $[0, T]$  given  $W_T = Y$ . If no jump occurs, then  $I = 1$  and the proposal  $Y$  is accepted as a sample from  $f_{Y_T}$ . Otherwise the proposal is rejected and one starts all over. The jump times of  $V$  can be generated exactly if  $0 \leq \phi(x) \leq \pi$  for some  $\pi > 0$ . In this case, the jump times are obtained by thinning a Poisson process with intensity  $\pi$ . A candidate Poisson arrival time  $t$  is accepted as an arrival time of  $V$  with probability  $\phi(W_t)/\pi$ , where  $W_t$  is sampled from a Brownian bridge given the end point  $W_T = Y$ .

The scope of the scheme is limited to those diffusions  $Y$  for which  $\phi$  is bounded and  $\mu_Y$  satisfies the required boundedness and Novikov conditions. To treat a wider class of

diffusion processes, Chen (2009) decomposes  $Y$  into bounded segments, and applies the acceptance/rejection mechanism to each of these segments. Our sampling scheme for a jump-diffusion builds on this localization approach. To detail the idea for the first segment of  $Y$ , select  $\theta > 0$  such that  $-\theta > \underline{y}$  and  $\theta < \bar{y}$  and consider  $\zeta = \inf\{t \geq 0 : |Y_t| \geq \theta\}$ , the exit time of  $Y$  from  $[-\theta, \theta]$ . The acceptance/rejection mechanism is used to sample the pair  $(\zeta, Y_\zeta)$ . The proposal pair is  $(\tau, W_\tau)$ , where  $\tau = \inf\{t \geq 0 : |W_t| \geq \theta\}$  is the exit time of a standard Brownian motion from  $[-\theta, \theta]$ . The proposal pair is easy to generate: Burq & Jones (2008) show how to sample  $\tau$  using an acceptance/rejection mechanism, and  $W_\tau$  is either  $-\theta$  or  $\theta$ , with equal probability. The likelihood ratio (LR) between the law of target pair and the law of the proposal pair is proportional to

$$\exp(A(W_\tau))\mathbb{E}\left[\exp\left(-\int_0^\tau \phi(W_s)ds\right)\middle|\tau, W_\tau\right] \quad (16)$$

where  $A$  is given by (13) and  $\phi$  is given by (15). Assuming that  $\phi(W) \geq 0$ , the expectation in the LR (16) is equal to the conditional probability that no arrivals occur during the interval  $[0, \tau]$  in a doubly-stochastic Poisson process  $V$  with intensity  $\phi(W)$ , given  $(\tau, W_\tau)$ . Assumption 2.1 suffices to guarantee continuity of  $\mu_Y$ , and hence boundedness of  $\phi(W_s)$  for  $s \in [0, \tau]$ . Thus the event times of  $V$  can be generated by thinning a dominating Poisson process. This now involves the sampling of values of  $W_s$  from a Brownian meander given  $(\tau, W_\tau)$ . Moreover, the function  $\exp(A(y))$  is bounded by a constant  $K$  because  $\mu_Y$  is continuous. This, together with the boundedness of  $\phi(W_s)$ , facilitates the generation of the Bernoulli indicator required for the acceptance test of the proposal pair  $(\tau, W_\tau)$ . A proposal is accepted as  $(\zeta, Y_\zeta)$  if  $V$  has no arrivals in the interval  $[0, \tau]$  and  $U \leq \exp(A(W_\tau))/K$ , where  $U$  is a random variable with uniform distribution on  $[0, 1]$ . If the proposal is rejected, one iterates. If the proposal is accepted, another level  $\theta$  is selected and the next segment of  $Y$  is generated. This procedure is repeated until the simulation horizon  $T$  is reached. Note that if the sampled  $\tau$  exceeds  $T$ , then the proposal pair is taken to be  $(\tau, W_T)$  and the target pair is  $(\zeta, Y_T)$ . The LR for the corresponding acceptance test is given by (16) with integration range  $[0, T]$  and  $W_\tau$  replaced by  $W_T$ .

### 3.2 Introducing jumps

We extend the acceptance/rejection scheme described above to a jump-diffusion process  $Y = F(X)$  solving (7), generated by a jump-diffusion process  $X$  satisfying Assumptions 2.1 and 2.2. Before stating the general algorithm, we explain the procedure for the first segment of  $Y$ . Thus, the goal is to draw a sample of  $Y_{T_1}$ .

Consider a process  $\bar{Y}$  solving the SDE

$$d\bar{Y}_t = \mu_Y(\bar{Y}_t)dt + dW_t, \quad (17)$$

with initial condition  $\bar{Y}_0 = Y_0$ . Clearly, if  $T_1$  is the first jump time of the process  $Y$ , then

$\bar{Y}_t \stackrel{d}{=} Y_t$  for  $0 \leq t < T_1$ . Define  $\zeta = \inf\{t \geq 0 : |\bar{Y}_t| \geq \theta\}$  for some level  $\theta$ , and observe that we can obtain a sample of  $Y_{T_1 \wedge \zeta}$  by sampling  $\bar{Y}_{T_1 \wedge \zeta}$ . Indeed, if  $T_1 > \zeta$ , then  $Y_t \stackrel{d}{=} \bar{Y}_t$  for all  $t \leq \zeta$ . If  $T_1 < \zeta$ , then  $Y_t \stackrel{d}{=} \bar{Y}_t$  for  $t < T_1$ . Thus, we can sample  $Y_{T_1}$  by sampling  $\bar{Y}_{T_1-}$  and adding the jump  $\Delta_Y(\bar{Y}_{T_1-}, Z_1)$ , where  $Z_1$  is a sample of the mark at  $T_1$ .

We start by generating a pair  $(\tau, W_\tau)$  for some level  $\theta$ , as in the diffusion case. Suppose  $\tau \leq T$ . Next we determine whether  $Y$  jumps during the interval  $[0, \tau]$ . To this end, we sample candidate jump times  $\nu_1, \dots, \nu_a \leq \tau$  from a Poisson process with intensity  $\pi$ , where  $\pi \geq \Lambda(F^{-1}(y))$  for  $y \in [-\theta, \theta]$ . In view of Assumption 2.1, a finite  $\pi$  exists because  $\bar{Y}_t$  does not leave the interval  $[-\theta, \theta]$  for  $t \in [0, \zeta]$ . A candidate jump time  $\nu_n$  is accepted as a jump time of  $Y$  with probability  $\Lambda(F^{-1}(W_{\nu_n}))/\pi$ , where  $W_{\nu_n}$  is drawn from a Brownian meander given  $(\tau, W_\tau)$ . We distinguish two cases: either none of the candidate jump times is accepted, or we accept at least one jump time. In the former case, we test the proposal skeleton  $(\tau, W_{\nu_1}, \dots, W_{\nu_a}, W_\tau)$ . Otherwise, we test the proposal skeleton  $(\tau, W_{\nu_1}, \dots, W_{\nu_\ell})$ , where  $\nu_\ell$  is the first candidate time that was accepted. Letting  $\eta = \tau \wedge \nu_\ell$ , with the convention that  $\nu_\ell = \infty$  if no candidate time was accepted, we will prove in Proposition A.1 that the LR required for the acceptance test is proportional to

$$\exp(A(W_\eta))\mathbb{E} \left[ \exp \left( - \int_0^\eta \phi(W_s) ds \right) \mid \tau, W_{\nu_1}, \dots, W_\eta \right] \quad (18)$$

where  $A$  is given by (13) and  $\phi$  is given by (15). Given the LR (18), the test is analogous to that in the diffusion case. If the proposal pair passes the test, it is a sample of  $(\zeta, Y_{\nu_1}, \dots, Y_{\nu_a}, Y_\zeta)$  or  $(\zeta, Y_{\nu_1}, \dots, Y_{\nu_{\ell-1}}, Y_{\nu_\ell-})$ , respectively. In the case that  $Y$  jumps at  $\nu_\ell$ , we draw a mark  $Z_1$  from the appropriate distribution and evaluate  $Y_{T_1} = Y_{\nu_\ell-} + \Delta_Y(Y_{\nu_\ell-}, Z_1)$ . We then proceed to generate the next segment of  $Y$ , starting from  $Y_\zeta$  or  $Y_{T_1}$ , respectively. Figure 1 illustrates the method.

### 3.3 Basic jump-diffusion algorithm

We state the exact algorithm for sampling a value  $Y_T$  of the jump-diffusion  $Y$  solving (7). The domain of  $Y$  is  $D_Y = (\underline{y}, \bar{y})$ . The initial conditions are:  $n = 1$ ,  $y = Y_0 = 0$  and  $s_0 = 0$ . Figure 2 provides a flow chart. Section 5 discusses the implementation.

1. Select  $\theta_n > 0$  such that  $\underline{y} + \theta_n < y < \bar{y} - \theta_n$ . See Section 5.4.  
 Sample  $\tau = \inf\{t \geq 0 : |W_t| \geq \theta_n\}$ . See Section 5.1.  
 Select  $\pi > 0$  such that  $\pi \geq \Lambda(F^{-1}(\bar{Y}_t))$  for  $t \in [s_{n-1}, \zeta_n]$ . Here,  $\zeta_n = \inf\{t \geq s_{n-1} : \bar{Y}_t \notin [y - \theta_n, y + \theta_n]\}$  where  $\bar{Y}_t$  solves the SDE (17) for  $t \geq s_{n-1}$  with  $\bar{Y}_{s_{n-1}} = y$ .
2. Sample event times  $\nu_1 < \dots < \nu_a \leq \tau \wedge (T - s_{n-1})$  of a Poisson process with rate  $\pi$ .  
 Sample event times  $\kappa_1 < \dots < \kappa_b \leq \tau \wedge (T - s_{n-1})$  of a Poisson process with rate  $M - m$ , where  $M$  is the max and  $m$  is the min of  $\phi(y + z)$  over  $z \in [-\theta_n, \theta_n]$ .

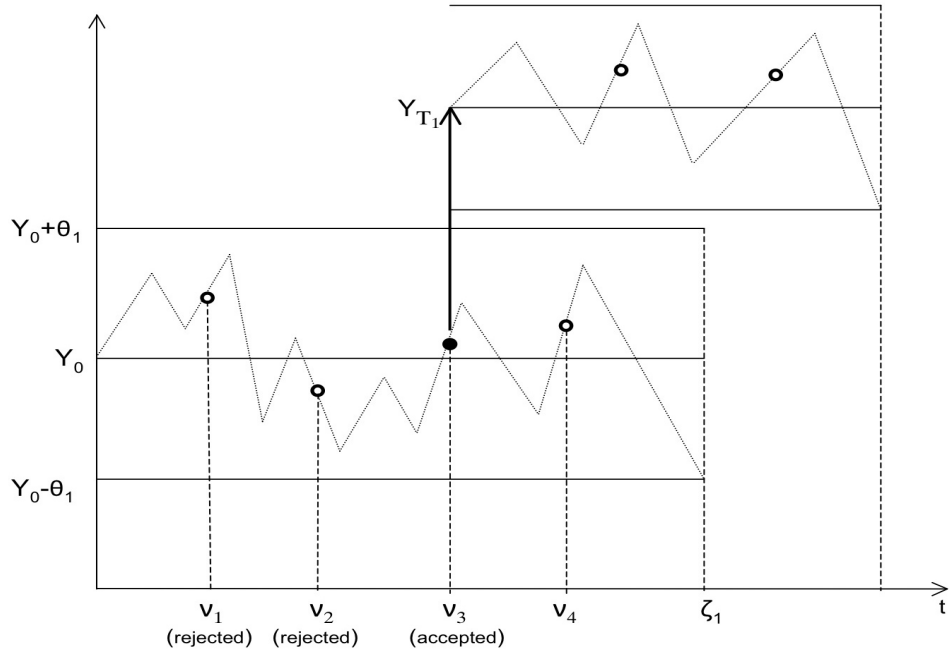


Figure 1: Generating the first jump time  $T_1$  and value  $Y_{T_1}$  of the jump-diffusion  $Y$ .

3. Sample  $(W_{\nu_1}, \dots, W_{\nu_a}, W_{\kappa_1}, \dots, W_{\kappa_b}, W_\tau, W_{\tau \wedge (T - s_{n-1})})$ . See Section 5.2.
4. Set  $i = 1$ . Loop:
  - Draw  $U_i \sim U(0, 1)$
  - If  $U_i \leq \Lambda(F^{-1}(Y_{s_{n-1}} + W_{\nu_i}))/\pi$ , then exit loop, set  $\ell = i$  and go to Step 6
  - If  $i = a$ , then exit loop and go to Step 5
  - Set  $i = i + 1$
5. Accept/reject the proposal skeleton  $(s_{n-1} + \tau, y + W_{\nu_1}, \dots, y + W_{\nu_a}, y + W_{\tau \wedge (T - s_{n-1})})$  as a sample of the skeleton  $(\zeta_n, Y_{s_{n-1} + \nu_1}, \dots, Y_{s_{n-1} + \nu_a}, Y_{(s_{n-1} + \tau) \wedge T})$  using the Poisson arrival times  $\kappa_j$  generated at Step 2. See Section 5.3.
  - If the proposal is accepted and  $T < s_{n-1} + \tau$ , return  $Y_T$  and stop. If the proposal is accepted and  $T > s_{n-1} + \tau$ , set  $y = Y_{s_{n-1} + \tau}$ ,  $s_n = \zeta_n = s_{n-1} + \tau$ ,  $n = n + 1$ . Go to Step 1.
  - If the proposal is rejected, go to Step 1.
6. Accept/reject the proposal skeleton  $(s_{n-1} + \tau, y + W_{\nu_1}, \dots, y + W_{\nu_\ell})$  as a sample of the skeleton  $(\zeta_n, Y_{s_{n-1} + \nu_1}, \dots, Y_{s_{n-1} + \nu_{\ell-1}}, Y_{(s_{n-1} + \nu_\ell)-})$  using the Poisson arrival times  $\kappa_j$  generated at Step 2. See Section 5.3.
  - If the proposal is accepted, draw a variable  $Z$  from the mark distribution  $\Pi$ . Set  $s_n = s_{n-1} + \nu_\ell$ ,  $y = Y_{s_n} = Y_{(s_{n-1} + \nu_\ell)-} + \Delta_Y(Y_{(s_{n-1} + \nu_\ell)-}, Z)$ ,  $n = n + 1$ . Go to Step 1.

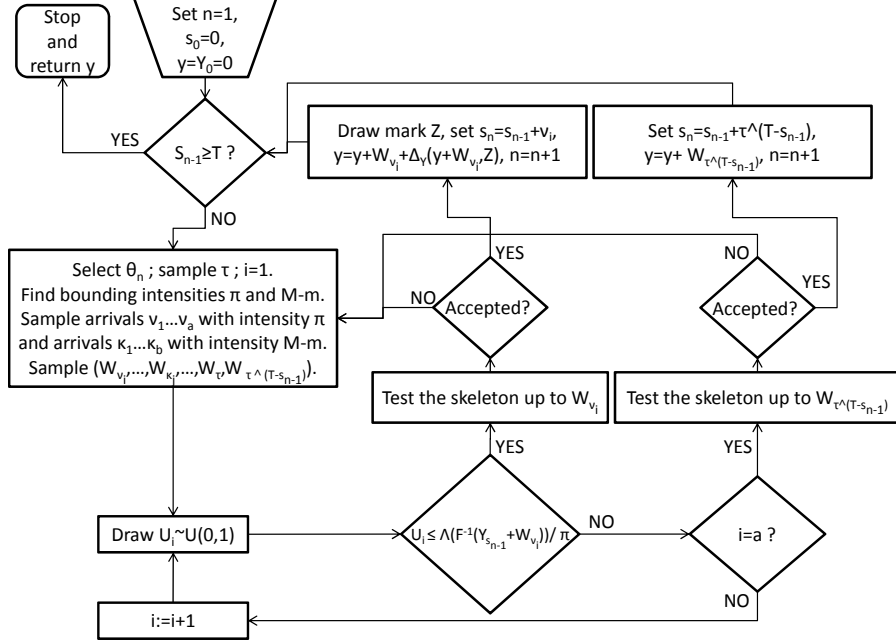


Figure 2: The basic jump-diffusion algorithm.

If the proposal is rejected, go to Step 1.

Note that a bound  $\pi$  in Step 1 exists because  $\Lambda$  is locally bounded, and because  $\bar{Y}_t$  is bounded for  $t \in [s_{n-1}, \zeta_n]$  and so is  $F^{-1}(\bar{Y}_t)$ . For Step 2, note that  $\phi(y+z)$  is bounded in  $z \in [-\theta_n, \theta_n]$  due to Assumption 2.1.

Not all the samples of  $(\nu_i, W_{\nu_i})$  generated at Steps 2 and 3 may actually be used in the subsequent steps. If, for example, the first candidate time  $\nu_1$  is accepted as a jump time of  $Y$  at Step 4, we exit the loop with  $\ell = 1$  and proceed to Step 6. The values  $(\nu_i, W_{\nu_i})_{2 \leq i \leq a}$  are no longer needed. To avoid the generation of excess samples, we could integrate Steps 2 to 4 into a loop. This would involve the sequential sampling of pairs  $(\nu_i, W_{\nu_i})$  until a candidate jump time  $\nu_i$  is accepted or the time  $\tau \wedge (T - s_{n-1})$  is reached. We settle on a non-sequential formulation because the sampling of a Brownian meander value  $W_{\nu_i}$  given the previous values  $(W_{\nu_j})_{j < i}$  and the exit time pair  $(\tau, W_\tau)$  is more expensive than the sampling of the entire vector of values of  $W_{\nu_i}$  in a single step.

The algorithm returns exact samples of the jump times  $T_1, \dots, T_{N_T}$  along with the values  $(Y_{T_1-}, Y_{T_1}), \dots, (Y_{T_{N_T}-}, Y_{T_{N_T}})$  and  $Y_T$ . By applying the inverse Lamperti transform  $F^{-1}$ , we obtain the corresponding values  $(X_{T_1-}, X_{T_1}), \dots, (X_{T_{N_T}-}, X_{T_{N_T}})$  and  $X_T$ . These samples are exact whenever  $F^{-1}$  can be evaluated exactly. The jump magnitudes of  $X$  are given by  $\Delta(X_{T_n-}, Z_n) = X_{T_n} - X_{T_n-}$ , and these values along with the  $T_n$  lead to an exact sample of a complete path  $(J_t)_{t \leq T}$  of the jump process (2).

## 4 Extensions

This section discusses several extensions of the basic jump-diffusion algorithm.

### 4.1 Sampling a jump-diffusion skeleton

The exact algorithm developed in Section 3.3 generates a sample of  $X_T$  for a fixed horizon  $T$ . It is straightforward to extend the algorithm to generate a skeleton of  $X$ , i.e., the values  $(X_t)_{t \in S}$  for a discrete set  $S$  of fixed times  $t \in [0, T]$ . This extension facilitates the treatment of certain path-dependent payoff functionals, such as those associated with discretely monitored Asian options.

It suffices to generate the values  $(Y_t)_{t \in S}$  and apply the inverse transform  $F^{-1}$ . To this end, we sample the values  $(W_t)_{t \in S}$  along with the values  $(W_{\nu_i})$  and  $(W_{\kappa_j})$  at Step 3. The proposal skeleton tested at Steps 5 or 6 then includes the values  $(W_t)_{t \in S}$ . The acceptance test itself remains unchanged, and is still based on the values  $W_{\kappa_j}$  only, see Section 5.3. The additional computational effort associated with generating a skeleton rather than a single value of  $X$  is minor, and consists only of the effort required to sample the  $(W_t)_{t \in S}$ .

### 4.2 Sampling a jump-diffusion hitting time and value

The exact algorithm can also be used to generate exact samples of a hitting time  $\xi$  of  $X$  to a fixed level and the corresponding value  $X_\xi$ . This extension facilitates the treatment of payoff functionals involving the hitting time, such as those associated with barrier options. It also allows us to address a range of other hitting time problems, for example the computation of default probabilities and corporate security values in a first-passage structural model with jump-diffusion firm value  $X$ . The ability to generate the value  $X_\xi$  facilitates the treatment of a model formulation with random recovery given by a fraction of the firm value at default.

To sample a hitting time, we only need to select the value of the level  $\theta_n$  appropriately. To illustrate, suppose we wish to generate a sample of  $\xi = \xi(x) = \inf\{t \leq T : X_t \leq x\}$  for a level  $x < X_0$ . Let  $\theta_n = \theta_n(y)$  be the value of the level  $\theta_n$  in the algorithm stated in Section 3.3. Then, to generate  $\xi$  along with the other variables, instead of taking  $\theta_n(y)$  as the level at Step 1 of the algorithm, we take  $\theta_n(y) \wedge (y - F(x))$ .

The process  $X$  can hit the level  $x$  either by a jump or by drift. If it jumps through  $x$  at, say, time  $T_n$ , we know that  $\xi(x) = T_n$ . The value  $Y_{\xi(x)} = Y_{T_n-} + \Delta_Y(Y_{T_n-}, Z_n)$  is generated at Step 6 of the algorithm along with all other variables. If the process hits  $x$  by drift, then  $\xi$  is the first time  $\zeta_i$  such that  $Y_{\zeta_i} = F(x)$ , and the corresponding value  $Y_{\xi(x)} = Y_{\zeta_i}$  is generated at Step 5 of the algorithm as the process value at the exit time. The inverse Lamperti transform finally gives  $X_\xi = F^{-1}(Y_\xi)$ .

### 4.3 Exponential of time-integrated jump-diffusion

A modification of the exact algorithm developed in Section 3.3 can be used to obtain an unbiased estimator of the expectation

$$B(T) = \mathbb{E} \left[ \exp \left( - \int_0^T X_s ds \right) u((X_t)_{t \in S}, (J_t)_{t \leq T}) \right] \quad (19)$$

where  $u$  is an integrable function and  $S$  is a discrete set of fixed times in  $[0, T]$ . Taking the jump-diffusion  $X$  as a model of the short-term interest rate,  $B(T)$  could represent the value of a fixed-income security such as a bond.

While we cannot generate the complete path of  $X$  between 0 and  $T$  in order to evaluate  $\exp(-\int_0^T X_s ds)$  exactly, we can nevertheless obtain an unbiased estimator of  $B(T)$  by taking advantage of its special structure. To see this, take  $u = 1$ . Then  $B(T)$  can be regarded as the probability that no arrivals occur during the interval  $[0, T]$  in a doubly-stochastic Poisson process with intensity  $X$ , provided that  $X \geq 0$ . Now suppose  $X$  is bounded on  $[0, T]$ . Then this probability can be estimated using the thinning procedure. For upper and lower bounds  $H$  and  $h$  on  $X$ , we sample arrival times  $(\varepsilon_k)$  on  $[0, T]$  of a Poisson process with rate  $H - h$ , and obtain the exact estimator  $e^{-hT} \prod_{k=1}^n (1 - \frac{X_{\varepsilon_k} - h}{H - h})$  of  $\exp(-\int_0^T X_s ds)$ , where  $n$  is the number of Poisson arrivals, and the  $X_{\varepsilon_k}$  are the exact samples of  $X$  at the Poisson arrival times.

We state the general algorithm, taking  $u = 1$  for ease of exposition. We emphasize that  $X$  is not required to be uniformly bounded. The initial conditions are  $n = 1$ ,  $y = Y_0 = 0$ ,  $s_0 = 0$  and  $g = 1$ . The estimator is denoted  $g$ .

1. Select  $\theta_n > 0$  such that  $\underline{y} + \theta_n < y < \bar{y} - \theta_n$ . See Section 5.4. Let  $\zeta_n = \inf\{t \geq s_{n-1} : \bar{Y}_t \notin [y - \theta_n, y + \theta_n]\}$  where  $\bar{Y}_t$  solves the SDE (17) for  $t \geq s_{n-1}$  with  $\bar{Y}_{s_{n-1}} = y$ .  
Select  $\pi > 0$  such that  $\pi \geq \Lambda(F^{-1}(\bar{Y}_t))$  for  $t \in [s_{n-1}, \zeta_n]$ .  
Sample  $\tau = \inf\{t \geq 0 : |W_t| \geq \theta_n\}$ . See Section 5.1.
2. Sample event times  $\nu_1 < \dots < \nu_a \leq \tau \wedge (T - s_{n-1})$  of a Poisson process with rate  $\pi$ .  
Sample event times  $\kappa_1 < \dots < \kappa_b \leq \tau \wedge (T - s_{n-1})$  of a Poisson process with rate  $M - m$ , where  $M$  is the max and  $m$  is the min of  $\phi(y + z)$  over  $z \in [-\theta_n, \theta_n]$ .  
Sample event times  $\varepsilon_1 < \dots < \varepsilon_c \leq \tau \wedge (T - s_{n-1})$  of a Poisson process with rate  $H - h$ , where  $H$  is the max and  $h$  is the min of  $F^{-1}(y + z)$  over  $z \in [-\theta_n, \theta_n]$ .
3. Sample  $(W_{\nu_1}, \dots, W_{\nu_a}, W_{\kappa_1}, \dots, W_{\kappa_b}, W_{\varepsilon_1}, \dots, W_{\varepsilon_c}, W_\tau, W_{\tau \wedge (T - s_{n-1})})$ . See Section 5.2.
4. Set  $i = 1$ . Loop:  
Draw  $U_i \sim U(0, 1)$   
If  $U_i \leq \Lambda(F^{-1}(Y_{s_{n-1}} + W_{\nu_i}))/\pi$ , then exit loop, set  $\ell = i$  and go to Step 6  
If  $i = a$ , then exit loop and go to Step 5  
Set  $i = i + 1$

5. Accept/reject the proposal skeleton  $(s_{n-1} + \tau, y + W_{\nu_1}, \dots, y + W_{\nu_a}, y + W_{\tau \wedge (T - s_{n-1})})$  as a sample of the skeleton  $(\zeta_n, Y_{s_{n-1} + \nu_1}, \dots, Y_{s_{n-1} + \nu_a}, Y_{(s_{n-1} + \tau) \wedge T})$  using the Poisson arrival times  $\kappa_j$  generated at Step 2. See Section 5.3.

If the proposal is accepted and  $T < s_{n-1} + \tau$ , set  $g = g \cdot e^{-h(T - s_{n-1})} \prod_{k=1}^c (1 - \frac{F^{-1}(y + Y_{\varepsilon_k}) - h}{H - h})$ , return  $g$  and stop. If the proposal is accepted and  $T > s_{n-1} + \tau$ , set  $g = g \cdot e^{-h\tau} \prod_{k=1}^c (1 - \frac{F^{-1}(y + Y_{\varepsilon_k}) - h}{H - h})$ . Set  $y = Y_{s_{n-1} + \tau}$ ,  $s_n = \zeta_n = s_{n-1} + \tau$ ,  $n = n + 1$ . Go to Step 1.

If the proposal is rejected, go to Step 1.

6. Accept/reject the proposal skeleton  $(s_{n-1} + \tau, y + W_{\nu_1}, \dots, y + W_{\nu_\ell})$  as a sample of the skeleton  $(\zeta_n, Y_{s_{n-1} + \nu_1}, \dots, Y_{s_{n-1} + \nu_{\ell-1}}, Y_{(s_{n-1} + \nu_\ell)-})$  using the Poisson arrival times  $\kappa_j$  generated at Step 2. See Section 5.3.

If the proposal is accepted, find  $c_0 = \sup\{k : \varepsilon_k < \nu_\ell\}$  and set  $g = g \cdot e^{-h\nu_\ell} \prod_{k=1}^{c_0} (1 - \frac{F^{-1}(y + Y_{\varepsilon_k}) - h}{H - h})$ . Draw a variable  $Z$  from the mark distribution  $\Pi$ . Set  $s_n = s_{n-1} + \nu_\ell$ ,  $y = Y_{s_n} = Y_{(s_{n-1} + \nu_\ell)-} + \Delta_Y(Y_{(s_{n-1} + \nu_\ell)-}, Z)$ ,  $n = n + 1$ . Go to Step 1.

If the proposal is rejected, go to Step 1.

## 4.4 Other extensions

The exact algorithms extend to the case of a more general jump intensity specification  $\lambda_t = \Lambda(X_{t-}, J_{t-}, N_{t-}, t)$  where  $\Lambda : D_X \times D_X \times \mathbb{N} \times [0, \infty) \rightarrow [0, \infty)$ . This formulation allows for an explicit dependence of the intensity on the jump component of  $X$ , and the modeling of a seasonal behavior of the jump frequency. The explicit time dependence may also be useful in model calibration, where it generates additional fitting flexibility. The dependence on the jump component allows one to control the jump behavior as a function of the jump state. For example, the jump intensity may be set to 0 after a specified number of jumps. The algorithm in Section 3.3 remains valid as stated under this more general formulation, because it proceeds sequentially between the jump times of  $X$  and the point process  $(J, N)$  is constant between these jump times.

Moreover, the algorithms extend to the case of a jump size function of the form  $\Delta(X_{T_n-}, J_{T_n-}, Z_n, T_n)$  where  $\Delta : D_X^2 \times E \times [0, \infty) \rightarrow D_X$ . This formulation allows for an explicit dependence of the size of the jump of  $X$  at  $T_n$  on the value of  $T_n$ , as well as the dependence on the value of the jump process just before the jump. The algorithm remains valid as stated under this generalization.

## 5 Implementation

This section discusses the implementation of each of the non-trivial steps of the exact algorithm described in Section 3.3. We begin by explaining the generation of a Brownian exit time  $\tau$  and end by discussing the selection of the level  $\theta_n$ .

## 5.1 Sampling Brownian exit times

The sampling of an exit time  $\tau$  at Step 1 follows Burq & Jones (2008), and is based on the self-similarity property of  $W$ . Since  $\theta W_{t/\theta^2} \stackrel{d}{=} W_t$ , we have  $\tau \stackrel{d}{=} \theta^2 \tau_1$ , where  $\tau_1 = \inf\{t \geq 0 : |W_t| = 1\}$ . The probability density function  $h(t)$  of  $\tau_1$  takes the form

$$\frac{1}{\sqrt{2\pi t^3}} e^{-\frac{1}{2t}} + \sum_{j=1}^{\infty} \frac{(-1)^j}{\sqrt{2\pi t^3}} \left[ (2j+1) \exp\left(-\frac{(2j+1)^2}{2t}\right) - (2j-1) \exp\left(-\frac{(2j-1)^2}{2t}\right) \right].$$

We can sample from  $h$  by acceptance/rejection. The density can be bounded from above by a Gamma density:  $h(t) \leq ag(t; b; \gamma) = a\gamma^b t^{b-1} e^{-\gamma t} / \Gamma(b)$ , where  $\Gamma$  is the Gamma function,  $a = 1.243707$ ,  $b = 1.088870$  and  $\gamma = 1.233701$ . We generate a sample  $v$  from  $g(t; b; \gamma)$  and accept  $v$  as a sample of  $\tau_1$  if  $aUg(v; b; \gamma) \leq h(v)$  for  $U \sim U(0, 1)$ .

The density  $h$  cannot be computed exactly. However, following Burq & Jones (2008), the acceptance test can still be performed by exploiting a special (oscillating) structure of the infinite sum. It suffices to find an integer  $n$  such that  $aUg(v; b; \gamma) < h^{n+1}(v) < h^n(v)$  to ensure that  $aUg(v; b; \gamma) < h(v)$ , where  $h^i$  represents the  $i$ th partial sum in the expansion of  $h$ . Similarly, if  $aUg(v; b; \gamma) > h^{n+1}(v) > h^n(v)$  then  $aUg(v; b; \gamma) > h(v)$ . Burq & Jones (2008) prove that the number of operations required to find this  $n$  is finite.

## 5.2 Sampling Brownian meanders

Given  $\tau$ , we need to generate  $W_\tau$ . This is trivial because  $\mathbb{P}(W_\tau = \theta) = \mathbb{P}(W_\tau = -\theta) = 1/2$ . Next, given  $(\tau, W_\tau)$ , we generate  $(W_{t_1}, \dots, W_{t_n}, W_{\tau \wedge (T-s)})$  for  $t_i < \tau$ . We consider the problem of generating  $W_t$  given  $(\tau_1, W_{\tau_1})$  for  $0 \leq t \leq \tau_1$ , since the self-similarity property of  $W$  implies that for  $0 < t_1 < \dots < t_n < \tau = \tau_1 \theta^2$ ,

$$(W_{t_1}, \dots, W_{t_n} \mid \tau, W_\tau) \stackrel{d}{=} \theta(W_{t_1/\theta^2}, \dots, W_{t_n/\theta^2} \mid \tau_1, W_{\tau_1}). \quad (20)$$

It is shown by Williams (1970) that given  $(\tau_1, W_{\tau_1})$ , the process  $(W_t)_{t \leq \tau_1}$  evolves as a time-reversed Brownian meander. According to Imhof (1984), a Brownian meander can be decomposed into three independent Brownian bridges  $B^i$ , each evolving from 0 to 0 during the interval  $[0, \tau_1]$ . Chen (2009) exploits this decomposition to sample the values of  $W_t$  given the pair  $(\tau_1, W_{\tau_1})$ . Define

$$V_t = \begin{cases} 1 - W_{\tau_1-t}, & W_{\tau_1} = 1 \\ 1 + W_{\tau_1-t}, & W_{\tau_1} = -1 \end{cases} \quad (21)$$

$$B_t = ((t/\tau_1 + B_{\tau_1-t}^1)^2 + (B_{\tau_1-t}^2)^2 + (B_{\tau_1-t}^3)^2)^{1/2}. \quad (22)$$

According to Theorem 4.3 in Chen (2009),

$$\frac{\mathbb{P}(V_{t_1} \in dy_1, \dots, V_{t_n} \in dy_n \mid \tau_1, W_{\tau_1})}{\mathbb{P}(B_{t_1} \in dy_1, \dots, B_{t_n} \in dy_n)} \propto \prod_{i=1}^n p(t_i, y_i; t_{i+1}, y_{i+1}) q(t_1, y_1) 1_{(0,2)}(y_i) \quad (23)$$

for  $y_i \in \mathbb{R}$ , where

$$\begin{aligned} p(s, x; t, y) &= \frac{1 - \sum_{j=1}^{\infty} (\theta_j(s, x; t, y) - \vartheta_j(s, x; t, y))}{1 - \exp(-2xy/(t-s))} \\ q(s, x) &= 1 - \frac{1}{x} \sum_{j=1}^{\infty} (\rho_j(s, x) - \varrho_j(s, x)) \end{aligned} \quad (24)$$

and where

$$\begin{aligned} \theta_j(s, x; t, y) &= \exp\left(-\frac{2(2j-x)(2j-y)}{t-s}\right) + \exp\left(-\frac{2(2(j-1)+x)(2(j-1)+y)}{t-s}\right) \\ \vartheta_j(s, x; t, y) &= \exp\left(-\frac{2j(4j+2(x-y))}{t-s}\right) + \exp\left(-\frac{2j(4j-2(x-y))}{t-s}\right) \\ \rho_j(s, x) &= (4j-x) \exp\left(-\frac{4j(2j-x)}{s}\right) \\ \varrho_j(s, x) &= (4j+x) \exp\left(-\frac{4j(2j+x)}{s}\right). \end{aligned}$$

The expression for the likelihood ratio (23) facilitates an acceptance/rejection sampling strategy using a proposal skeleton  $(B_{t_1}, \dots, B_{t_n})$ . While the expression (23) cannot be evaluated exactly, Chen (2009) shows that the infinite sums in (24) satisfy an oscillating property that allows one to perform the acceptance test based on a finite number of summands. We summarize the steps required to generate  $(W_{t_1}, \dots, W_{t_n} \mid \tau)$ :

1. Sample  $W_{\tau_1}$  using that  $\mathbb{P}(W_{\tau} = 1) = \mathbb{P}(W_{\tau} = -1) = 1/2$ .
2. Sample the values  $(B_{t_1}^i, \dots, B_{t_n}^i)_{i=1,2,3}$  of Brownian bridges from 0 to 0 on  $[0, \tau_1]$ .
3. Transform these samples into a sample of  $(B_{\tau_1-t_1}, \dots, B_{\tau_1-t_n})$  using (22).
4. Generate  $n+1$  random variables  $U_j \sim U(0, 1)$ .

Accept  $(B_{\tau_1-t_1} \dots B_{\tau_1-t_n})$  as a sample of  $(V_{\tau_1-t_1} \dots V_{\tau_1-t_n})$  if

$$\begin{aligned} U_j &\leq p(\tau_1 - t_n, B_{\tau_1-t_n}; \tau_1 - t_{n+1}, B_{\tau_1-t_{n+1}}), \quad 1 \leq j \leq n \\ U_{n+1} &\leq q(\tau_1 - t_n, B_{\tau_1-t_n}). \end{aligned}$$

5. Transform  $V_{\tau_1-t}$  into  $W_t$  using (21).

6. Scale  $W_t$  using (20).

### 5.3 Acceptance test

We detail the acceptance test performed at Steps 5 and 6. Let  $\eta = \min(\tau, \nu_\ell, T - s)$ . Here,  $\nu_\ell$  is the first jump time candidate for  $Y$  accepted in Step 4, with the convention that  $\nu_\ell = \infty$  if no candidate jump time is accepted. By Proposition A.1 in the Appendix, the LR between the conditional law of the target skeleton

$$(\zeta_n - s_{n-1}, Y_{s_{n-1}+\nu_1} - Y_{s_{n-1}}, \dots, Y_{(s_{n-1}+\eta)-} - Y_{s_{n-1}}) \quad (25)$$

given  $(s_{n-1}, Y_{s_{n-1}})$  and the law of the proposal skeleton

$$(\tau, W_{\nu_1}, \dots, W_\eta) \quad (26)$$

is proportional to

$$L = \exp(A(Y_{s_{n-1}} + W_\eta)) \mathbb{E} \left[ \exp \left( - \int_0^\eta \phi(Y_{s_{n-1}} + W_u) du \right) \mid \tau, W_{\nu_1}, \dots, W_\eta \right]. \quad (27)$$

To ensure that the integrand in the expectation is non-negative, we let  $m$  be the lower bound  $\min_{z \in \Theta} \phi(Y_{s_{n-1}} + z)$  for  $\Theta = [-\theta_n, \theta_n]$  and we rewrite  $L$  as

$$L = \exp(A(Y_{s_{n-1}} + W_\eta)) \exp(-m\eta) \times \mathbb{E} \left[ \exp \left( - \int_0^\eta [\phi(Y_{s_{n-1}} + W_u) - m] du \right) \mid \tau, W_{\nu_1}, \dots, W_\eta \right]. \quad (28)$$

The conditional expectation in (28) is equal to the conditional probability that no arrivals occur during the interval  $[0, \eta]$  in a doubly-stochastic Poisson process  $H$  with intensity  $\phi(Y_{s_{n-1}} + W_u) - m$ , given  $(\tau, W_{\nu_1}, \dots, W_\eta)$ . The intensity is bounded above by  $M - m$  where  $M = \max_{z \in \Theta} \phi(Y_{s_{n-1}} + z)$ , allowing us to simulate the event times of  $H$  by thinning a Poisson process with intensity  $M - m$ . Moreover, the first term of  $L$  is bounded above by  $K = \max_{z \in \Theta} \exp(A(Y_{s_{n-1}} + z))$  and the second term is bounded above by  $S = \exp(-m(T - s_{n-1})) \vee 1$ . These properties facilitate the generation of the Bernoulli indicator for the acceptance test of a proposal skeleton (26).

From Step 2, we have arrival times  $\kappa_1 < \dots < \kappa_b < \eta$  of a Poisson process with rate  $M - m$ . From Step 3, we also have the corresponding values  $W_{\kappa_i}$  for  $i = 1, \dots, b$ . Now the acceptance test for a proposal skeleton proceeds as follows:

1. Draw  $U_i \sim U(0, 1)$  for  $1 \leq i \leq b + 2$ .

2. Accept a proposal skeleton (26) as a sample of (25) if

$$\begin{aligned} (M - m)U_i &> \phi(Y_{s_{n-1}} + W_{\kappa_i}) - m, \quad 1 \leq i \leq b, \\ KU_{b+1} &\leq \exp(A(Y_{s_{n-1}} + W_\eta)), \\ SU_{b+2} &\leq \exp(-m\eta). \end{aligned}$$

## 5.4 Level selection

We explain the selection of  $\theta_n$ . During the  $n$ th iteration, we generate

$$\eta = \min(\tau, \nu_\ell, T - s),$$

the minimum of the exit time from  $[Y_{s_{n-1}} - \theta_n, Y_{s_{n-1}} + \theta_n]$ , the first jump time of  $Y$  and the remaining time to the horizon  $T$ . Then we generate a proposal skeleton at a collection of times  $t_j$  such that  $0 < t_1 < t_2 < \dots < \eta$ . The pair of the proposal skeleton and  $\eta$  is tested subsequently, as explained in Section 5.3. If it is accepted, we iterate, starting from  $s_n = s_{n-1} + \eta$ . Assuming that the computational effort required to generate a proposal skeleton does not vary greatly with  $\eta$ , we wish to maximize both the time increment  $\eta$  and the probability of accepting the proposal skeleton. In other words, we wish to reach the horizon  $T$  as quickly as possible, while rejecting as few proposal skeletons as possible. Thus, letting  $P_A$  be the conditional probability of accepting a proposal skeleton (26) given the vector  $(Y_{s_{n-1}}, \tau, \nu_\ell, W_{\nu_1}, \dots, W_\eta)$ , we propose to select  $\theta = \theta_n$  so as to maximize

$$\mathcal{M}(\theta, Y_{s_{n-1}}) = \mathbb{E}[\eta P_A(Y_{s_{n-1}}, \tau, \nu_\ell, W_{\nu_1}, \dots, W_\eta) \mid Y_{s_{n-1}}] \quad (29)$$

Since it is difficult to compute the conditional expectation (29), we first develop a lower bound on (29) and then approximate this bound. The level  $\theta = \theta_n$  is selected as the maximizer of the estimator of the bound. Our numerical experiments in Section 6 indicate that this level selection procedure leads to an efficient algorithm. We also remark that the approximations introduced for the purpose of selecting  $\theta$  do not introduce bias into the simulation estimators.

Fix  $s = s_{n-1}$ . From the analysis in Section 5.3, for any proposed Brownian exit time  $\tau$ , the conditional acceptance probability satisfies

$$\begin{aligned} P_A(Y_s, \tau, \nu_\ell, W_{\nu_1}, \dots, W_\eta) &= \mathbb{P}(KU_1 \leq \exp(A(Y_s + W_\eta)) \mid Y_s, W_\eta) \mathbb{P}(SU_2 \leq \exp(-m\eta) \mid \tau, \nu_\ell) \\ &\quad \times \mathbb{P}(H_\eta - H_0 = 0 \mid Y_s, \tau, \nu_\ell, W_{\nu_1}, \dots, W_\eta) \\ &= \exp(A(Y_s + W_\eta)) K^{-1} \exp(-m\eta) S^{-1} \mathbb{P}(H_\eta - H_0 = 0 \mid Y_s, \tau, \nu_\ell, W_{\nu_1}, \dots, W_\eta) \end{aligned}$$

where the  $U_j$  are independent standard uniform variables,  $K$  and  $S$  are as in Section 5.3,

and  $H$  is a doubly-stochastic Poisson process with intensity  $\phi(Y_s + W_t) - m$  at  $t$ . Since  $H$  is dominated by a Poisson process with intensity  $M - m$ , a function of  $Y_s$ , we have

$$\begin{aligned} P_A(Y_s, \tau, \nu_\ell, W_{\nu_1}, \dots, W_\eta) &\geq \exp(A(Y_s + W_\eta))K^{-1} \exp(-m\eta)S^{-1} \exp(-(M - m)\eta) \\ &= \exp(A(Y_s + W_\eta) - M\eta)/(KS), \end{aligned}$$

where the lower bound is a function of  $(Y_s, \eta, W_\eta)$ . Thus we have

$$\begin{aligned} \mathcal{M}(\theta, Y_s) &\geq \mathbb{E}[\eta \exp(A(Y_s + W_\eta) - M\eta)/(KS) | Y_s] \tag{30} \\ &= \frac{1}{KS} \int \min(t, x, T - s) e^{A(Y_s + \omega) - M \min(t, x, T - s)} \mathbb{P}(\tau \in dt, \nu_\ell \in dx, W_\eta \in d\omega | Y_s). \end{aligned}$$

We approximate this lower bound on  $\mathcal{M}(\theta, Y_s)$  by approximating the joint conditional density of  $(\tau, \nu_\ell, W_\eta)$ . It is clear that

$$\begin{aligned} \mathbb{P}(\tau \in dt, \nu_\ell \in dx, W_\eta \in d\omega | Y_s) &= \mathbb{P}(W_\eta \in d\omega | \tau = t, \nu_\ell = x, Y_s) \mathbb{P}(\tau \in dt, \nu_\ell \in dx | Y_s) \\ &= \mathbb{P}(W_\eta \in d\omega | \tau = t, \nu_\ell = x) \mathbb{P}(\nu_\ell \in dx | Y_s) h(t) dt \end{aligned}$$

where  $h$  is the density of  $\tau$  given in Section 5.1 above. The exact computation of the probability  $\mathbb{P}(\nu_\ell \in dx | Y_s)$  is difficult. We approximate it by supposing that the jumps of  $Y$  occur according to a Poisson process with intensity  $c = c(Y_s) = \max_{z \in \Theta} \Lambda(F^{-1}((Y_s + z)))$ . This gives  $\mathbb{P}(\nu_\ell \in dx | Y_s) \approx c \exp(-cx) dx$ . It remains to compute the conditional distribution of  $W_\eta$ . If  $\min(t, x, T - s) = t$ , then the conditional distribution is known because  $\mathbb{P}(W_\tau = \theta) = \mathbb{P}(W_\tau = -\theta) = 1/2$ . If  $\min(t, x, T - s)$  is equal to either  $x$  or  $T - s$ , then the conditional distribution takes a more complicated form. In that case, we approximate it by a distribution that has unit mass at 0, the mean of the true distribution. More precisely, we take

$$\begin{aligned} \mathbb{P}(W_\eta \in d\omega | \tau = t, \nu_\ell = x) &= \frac{1}{2} (\delta(\omega - \theta) + \delta(\omega + \theta)) d\omega, \quad \min(t, x, T - s) = t \\ &\approx \delta(\omega) d\omega, \quad \min(t, x, T - s) = x \quad \text{or} \quad T - s, \end{aligned}$$

where  $\delta$  is the delta function. Thus, our estimator  $\widetilde{\mathcal{M}}_L(\theta, Y_s)$  of the lower bound (30) of

$\mathcal{M}(\theta, Y_s)$  takes the form

$$\begin{aligned}\widetilde{\mathcal{M}}_L(\theta, Y_s) &= \frac{c}{KS} \int_0^{T-s} \left( \int_0^t x e^{A(Y_s) - Mx - cx} dx \right) h(t) dt \\ &+ \frac{c}{KS} \int_0^{T-s} \left( \int_t^\infty \frac{1}{2} (e^{A(Y_s + \theta)} + e^{A(Y_s - \theta)}) e^{-cx} dx \right) e^{-Mt} h(t) dt \\ &+ \frac{c}{KS} \int_{T-s}^\infty \left( \int_0^{T-s} x e^{A(Y_s) - Mx - cx} dx \right) h(t) dt \\ &+ \frac{c}{KS} \int_{T-s}^\infty \left( \int_{T-s}^\infty e^{A(Y_s) - M(T-s) - cx} dx \right) (T-s) h(t) dt.\end{aligned}$$

The numerical calculation of the estimator  $\widetilde{\mathcal{M}}_L(\theta, Y_s)$  is straightforward. We choose  $\theta$  so as to maximize  $\widetilde{\mathcal{M}}_L(\theta, Y_s)$ . Instead of performing this optimization at the beginning of each iteration of the algorithm, we can build a table of optimal values  $\theta = \theta^*(y)$  for a range of values of  $y = Y_s \in D_Y$  before running the algorithm, and then take some interpolation between table values when running the algorithm.

## 6 Numerical tests for the JDCEV model

This section illustrates the behavior of the exact sampling scheme for the jump-to-default extended CEV (JDCEV) model of Carr & Linetsky (2006).

### 6.1 Specification

Suppose the jump-diffusion  $X$  describes the time evolution of the price of a share of stock under a risk-neutral measure  $\mathbb{P}$ . The SDE (1) takes the form

$$dX_t = (r + \Lambda(X_t))X_t dt + aX_t^{\beta+1} dW_t + dJ_t \quad (31)$$

where  $X_0 > 0$  is the initial stock price,  $r > 0$  is the risk-free rate,  $a > 0$  and  $\beta < 0$  are parameters, and the jump intensity and jump size functions are given by

$$\Lambda(x) = b + ca^2 x^{2\beta} \quad (32)$$

$$\Delta(x, z) = -x \quad (33)$$

for parameters  $b \geq 0$  and  $c \geq 1/2$ . The term  $\Lambda(X_t)X_t$  appearing in the drift compensates the jump process  $J$ , and ensures that the discounted stock price process defined by  $\exp(-rt)X_t$  is a martingale. The issuer of the stock defaults at  $T_1$ , the first jump time of  $X$ . The default intensity  $\lambda = \Lambda(X_-)$  is inversely related to the stock price, and grows without bound as the stock price decreases toward 0. At  $T_1$ , the stock price drops to 0

and remains there forever.

The domain of  $X$  is  $D_X = [0, \infty)$ , where 0 is an absorbing boundary. While the coefficient and intensity functions of  $X$  violate the usual Lipschitz and linear growth conditions, Carr & Linetsky (2006) prove that for  $c \geq 1/2$ , the SDE (31) has a unique strong solution, which cannot reach 0 or  $\infty$  with a drift, and can reach 0 only by a jump. Assumptions 2.1 and 2.2 are satisfied.

The model (31) provides some degree of analytical tractability. Carr & Linetsky (2006) develop closed formulas for the prices of European options written on  $X$ , default probabilities, and corporate bond values. Simulation can be used to analyze exotic options and other quantities for which analytical solutions are unavailable. The model is, however, a challenge for simulation. The SDE (31) falls outside the scope of the exact scheme of Casella & Roberts (2011) because the jump intensity is unbounded. It also falls outside the scope of the exact scheme of Giesecke et al. (2010) because the intensity and volatility functions are non-linear. However, the exact method of Section 3.3 and a discretization method apply. We contrast these methods. Unless noted otherwise, the model parameters values used are  $X_0 = 50$ ,  $\beta = -1$ ,  $r = 0.05$ ,  $a = 50/4$ ,  $b = 0$ , and  $c = 1/2$ ; these values are taken from Carr & Linetsky (2006).

## 6.2 Exact method

The exact scheme requires the computation of the Lamperti transform (5). For the specification (31), the Lamperti transform takes the form

$$F(x) = \begin{cases} (X_0^{-\beta} - x^{-\beta})/(a\beta), & x \in (0, \infty) \\ X_0^{-\beta}/(a\beta), & x = 0. \end{cases} \quad (34)$$

It maps  $D_X = [0, \infty)$  into  $D_Y = [X_0^{-\beta}/(a\beta), \infty)$ . The drift function (8) of the unit-volatility jump-diffusion  $Y = F(X)$  satisfying the SDE (7) is given by

$$\mu_Y(y) = \frac{1}{a}(r + b)(X_0^{-\beta} - ya\beta) + a \frac{c - (\beta + 1)/2}{X_0^{-\beta} - ya\beta}, \quad y \in (X_0^{-\beta}/(a\beta), \infty). \quad (35)$$

The jump size function (10) of  $Y$  takes the form

$$\Delta_Y(y, z) = F(0) - y = X_0^{-\beta}/(a\beta) - y, \quad y \in [X_0^{-\beta}/(a\beta), \infty). \quad (36)$$

Note that the boundary  $X_0^{-\beta}/(a\beta)$  of  $D_Y$  is absorbing, and can be attained only through a jump at  $T_1$ . The boundary  $\infty$  is unattainable. This mirrors the behavior of  $X$ .

### 6.3 Discretization method

A conventional discretization scheme approximates  $X$  on a discrete-time grid. Consider a partition of  $[0, T]$  into  $I$  segments of equal length  $h = T/I$ . The discretization  $\widehat{X}$  of  $X$  prior to its first jump time  $T_1$  is  $\widehat{X}_0 = X_0$  and, for  $i = 0, \dots, I - 1$ ,

$$\widehat{X}_{i+1} = \widehat{X}_i + (r + \Lambda(\widehat{X}_i))\widehat{X}_i h + a\widehat{X}_i^{\beta+1}\mathcal{N}_i, \quad (37)$$

where  $(\mathcal{N}_i)$  is a sequence of independent random variables, each of which has a normal distribution with mean 0 and variance  $h$ . The jump time  $T_1$  is taken as the minimum of  $\inf\{ih : i \geq 0, \widehat{X}_{i+1} \leq 0\}$  and  $\inf\{ih : i \geq 0, \widehat{C}_{i+1} \geq \mathcal{E}\}$ , where  $\mathcal{E}$  is an independent standard exponential random variable and  $\widehat{C}$  is a discretization of the compensator  $C = \int_0^\cdot \Lambda(X_s)ds$  to the jump counting process  $N$  given by  $\widehat{C}_0 = 0$  and

$$\widehat{C}_{i+1} = h \sum_{k=0}^i \Lambda(\widehat{X}_k), \quad i = 0, \dots, I - 1. \quad (38)$$

This time-scaling scheme for sampling  $T_1$  is based on a result of Meyer (1971), which implies that  $N$  can be transformed into a standard Poisson process by a change of time given by  $C$ . This, in turn, implies that  $T_1 \stackrel{d}{=} \inf\{t \geq 0 : C_t \geq \mathcal{E}\}$ .

### 6.4 European option

We begin by estimating the price of a European put option with strike price  $K$  and expiration date  $T$  written on  $X$ , given by

$$\exp(-rT)\mathbb{E}[(K - X_T)^+]. \quad (39)$$

Table 1 reports the simulation results for  $K = 5$  and  $T = 1$  year. The root mean square error (RMSE) is given by  $\sqrt{\text{SE}^2 + \text{Bias}^2}$ . The standard error (SE) is estimated as the sample standard deviation of the simulation output divided by the square root of the number of trials. The bias is given by the difference between the expectation of the estimator and the true value of the option. The bias of the estimator generated by the exact method is 0. The bias of the estimator generated by the discretization scheme is estimated using 10 million trials to estimate the expectation of the estimator, and then taking the difference with the true value, which is computed using the closed formulas developed by Carr & Linetsky (2006). Motivated by the results of Duffie & Glynn (1995), the number of discretization time steps  $I$  is set equal to the square-root of the number of simulation trials. Here and in other parts of the paper, the simulations were performed on a server with an Intel Core Duo 3.16 GHz processor and 4GB RAM. The codes were written in MATLAB Version 7.9.0.529 (R2009b).

Figure 3 shows the convergence of the RMSEs graphically. The exact method achieves

Method	Trials	Steps	Value	Bias	SE	RMSE	Time (sec)
Exact	10K	N/A	0.1398	0	0.0080	0.0080	34.4
	20K	N/A	0.1417	0	0.0057	0.0057	73.53
	40K	N/A	0.1449	0	0.0041	0.0041	141.96
	100K	N/A	0.1469	0	0.0026	0.0026	350.31
	500K	N/A	0.1495	0	0.0012	0.0012	1806.74
Discretization	10K	100	0.1417	0.0019	0.0081	0.0083	26.72
	20K	140	0.1496	0.0018	0.0059	0.0062	75.19
	40K	200	0.1422	0.0008	0.0042	0.0041	215.75
	100K	310	0.1531	0.0005	0.0027	0.0027	822.07
	500K	707	0.1478	0.0004	0.0012	0.0013	9373.81

Table 1: Simulation results under the model (31) for a European put option with strike price  $K = 5$  and expiration date  $T = 1$  year. The parameter values are  $X_0 = 50$ ,  $\beta = -1$ ,  $r = 0.05$ ,  $a = 50/4$ ,  $b = 0$ , and  $c = 1/2$ . The true value of the option is 0.1491.

the optimal square-root convergence: the error of the estimator decreases at the rate  $O(1/\sqrt{t})$ , where  $t$  is the computational budget. The convergence rate of the discretization scheme is slower, indicating that the discretization bias is significant. The exact method also outperforms the discretization scheme in terms of absolute errors: it generates the smallest RMSE for almost any computational budget considered.

We evaluate the performance of the methods for different parameter configurations. Figure 4 shows the error convergence rates for each of several parameter sets. Neither an increase in the CEV volatility parameter  $\beta$  from  $-1$  to  $-1/2$  nor an increase in the jump intensity sensitivity  $c$  from  $1/2$  to  $1$  has a material effect on the performance of the methods. A reduction of the initial value  $X_0$  from  $50$  to  $25$  as well as an increase of the intensity parameter  $b$  from  $0$  to  $0.2$  slows the exact algorithm down.

To understand the behavior of the algorithm for different parameter sets, consider the likelihood ratio (28). This ratio depends on the choice of localizing constant  $\theta$ , the drift  $\mu_Y(Y_t)$  of the unit-volatility process  $Y$ , and the function  $\phi = \mu_Y^2(Y_t) + \mu_Y'(Y_t)$ . Since the likelihood ratio depends on  $\exp(-\phi)$ , the likelihood ratio is lower for the subsets of  $D_Y$  corresponding to higher values of  $\phi$ . For example, the performance degrades when the starting value  $X_0$  is lowered because in this case the paths of the process more often hit the values close to zero, where  $\mu_Y$  is very large and acceptance rates are very low. It is, however, difficult to generally state how the drift, volatility, or jump intensity influence acceptance rates, because  $\mu_Y$  depends in a rather non-trivial way on  $\mu$ ,  $\sigma$  and their derivatives. The jump intensity does not affect the algorithm's acceptance ratios, but it still affects its performance. The more uniform the intensity is, the faster algorithm. In the opposite case, if the maximum and minimum of  $\Lambda(y)$  for  $y \in (Y_t - \theta, Y_t + \theta)$  differ significantly, many candidate arrival times will be wasted.

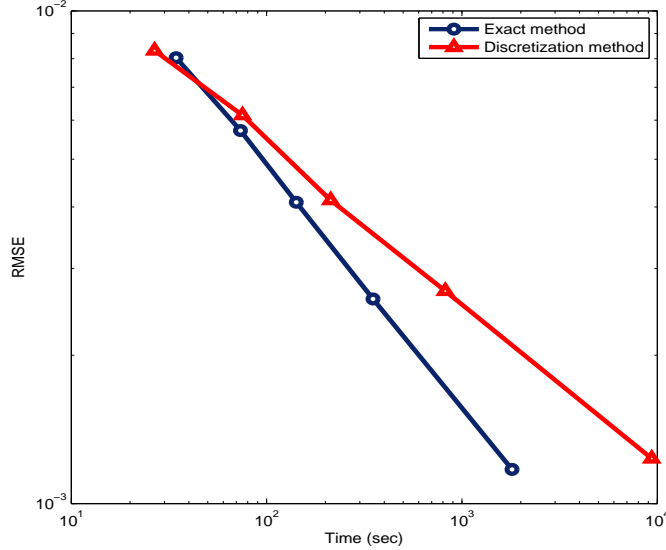


Figure 3: Convergence of the RMSEs for the European put option in Table 1.

## 6.5 Exotic options

While analytical solutions for the prices of European options written on the jump-diffusion (31) are available, analytical solutions for the prices of exotic options are not. The exact simulation method can be used to value many exotic options. To illustrate, we consider a discretely monitored Asian put option on (31). The price of this option is

$$\exp(-rT)\mathbb{E}\left[\left(K - \frac{1}{n}\sum_{i=1}^n X_{t_i}\right)^+\right] \quad (40)$$

where  $K$  is the strike price,  $T$  is the expiration date, and  $(t_i)_{i=1,\dots,n}$  is a sequence of monitoring dates. When evaluating (40), we exploit the ability of our method to generate an exact sample of a skeleton  $(X_{t_i})_{i=1,\dots,n}$ . Table 2 reports the results for semi-annual monitoring,  $K = 5$  and  $T = 1$  year. Figure 5 shows the convergence of the RMSEs. (The true value of the option needed for the computation of the bias of the discretization estimator was estimated using the exact method and 10 million trials.) The exact method achieves the optimal square-root convergence, while the convergence of the discretization scheme is slower. When the computational budget is relatively small, the discretization method achieves a somewhat smaller RMSE than the exact method. As the frequency of monitoring grows, the line representing the exact scheme is shifted further to the right while the line representing the discretization method remains fixed. This is because the run time of the exact scheme is increasing with the number of skeleton values that need to be sampled, while that of the discretization scheme remains roughly constant.

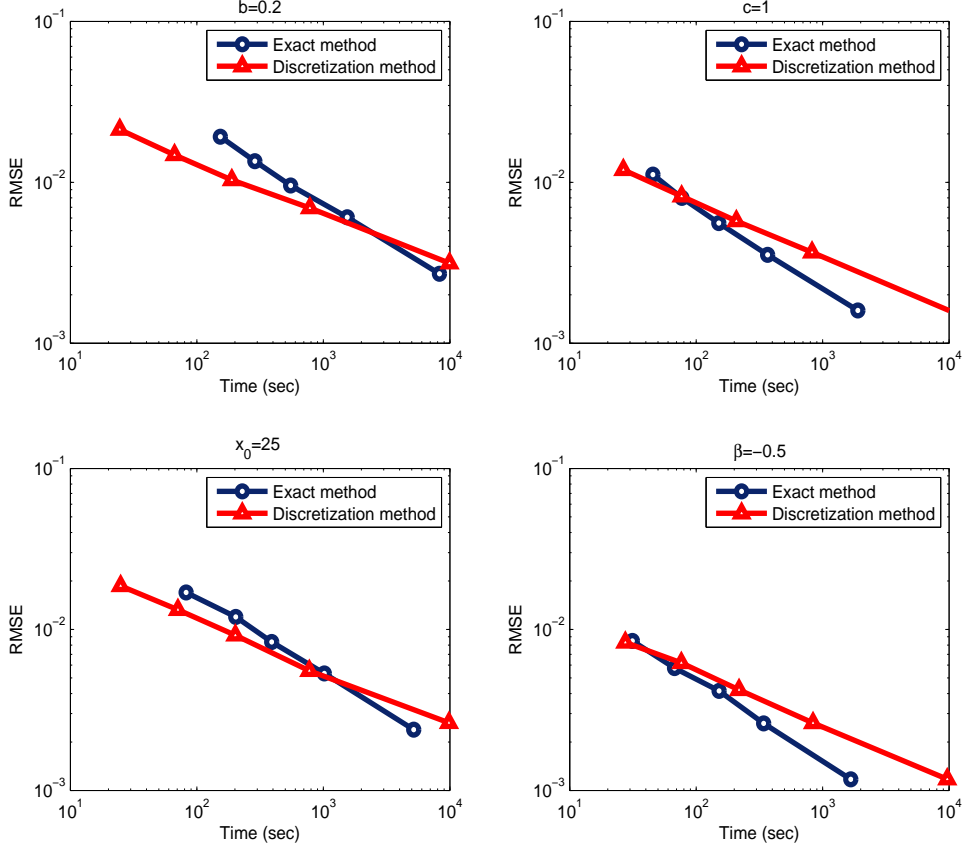


Figure 4: Convergence of the RMSEs for the European put option, for different parameter sets. The base parameters are  $X_0 = 50$ ,  $\beta = -1$ ,  $r = 0.05$ ,  $a = 50/4$ ,  $b = 0$ , and  $c = 1/2$ . Only one parameter is perturbed for each plot, as indicated.

Next consider a down-and-out call option with value

$$\exp(-rT)\mathbb{E}[(X_T - K)^+ 1_{\{\inf_{0 \leq t \leq T} X_t > B\}}] \quad (41)$$

where  $K$  is the strike price,  $B < X_0$  is the barrier, and  $T$  is the expiration date. To evaluate (41), we exploit the ability of our method to generate exact samples of the hitting time of  $X$  to  $B$ . Table 3 reports the results for  $K = 65$ ,  $B = 5$  and  $T = 1$  year. Figure 6 shows the convergence of the RMSEs. (The true value of the option needed for the computation of the bias of the discretization estimator was estimated using the exact method and 10 million trials.) The exact method achieves the optimal square-root convergence, while the convergence of the discretization scheme is slower. The exact method also achieves the smallest RMSE for any computational budget considered.

Method	Trials	Steps	Value	Bias	SE	RMSE	Time (sec)
Exact	10K	N/A	0.0728	0	0.0058	0.0058	46.71
	20K	N/A	0.0723	0	0.0041	0.0041	93.24
	40K	N/A	0.0809	0	0.0031	0.0031	188.88
	100K	N/A	0.0779	0	0.0019	0.0019	483.57
	500K	N/A	0.0738	0	0.0008	0.0008	2739.71
Discretization	10K	100	0.0837	0.0014	0.0063	0.0065	28.20
	20K	140	0.0725	0.0008	0.0041	0.0042	77.37
	40K	200	0.0754	0.0005	0.0030	0.0030	221.06
	100K	310	0.0740	0.0004	0.0019	0.0019	846.42
	500K	707	0.0747	0.0002	0.0008	0.0008	9664.92

Table 2: Simulation results under the model (31) for a semi-annually monitored Asian put option with strike price  $K = 5$  and expiration date  $T = 1$  year. The parameter values are  $X_0 = 50$ ,  $\beta = -1$ ,  $r = 0.05$ ,  $a = 50/4$ ,  $b = 0$ , and  $c = 1/2$ . The true value is 0.0745.

## 7 Numerical tests for an AJD model

This section illustrates the behavior of the exact sampling scheme for a model in the affine jump-diffusion (AJD) class of Duffie et al. (2000).

### 7.1 Specification

The process  $X$  describes the time evolution of the short-term rate of interest under a risk-neutral measure  $\mathbb{P}$ . The SDE (1) takes the form

$$dX_t = \kappa(\theta - X_t)dt + \sigma\sqrt{X_t}dW_t + dJ_t \quad (42)$$

where  $X_0 > 0$  is the initial short rate,  $\kappa, \theta > 0$  are mean-reversion speed and level parameters, and  $\sigma > 0$  is the diffusive volatility. For parameters  $\Lambda_0, \Lambda_1 \geq 0$ , the jump intensity and jump size functions are given by

$$\Lambda(x) = \Lambda_0 + \Lambda_1 x \quad (43)$$

$$\Delta(x, z) = z. \quad (44)$$

Taking  $2\kappa\theta > \sigma^2$ , the domain of  $X$  is  $D_X = (0, \infty)$ . The parameter values used in the numerical tests are  $X_0 = \theta = 0.0422$ ,  $\kappa = 0.0117$ ,  $\sigma = 0.0130$ ,  $\Lambda_0 = 0.0110$ ,  $\Lambda_1 = 0.1000$ , and a mark variable  $Z_n$  is drawn from a uniform distribution  $U(0.0113, 0.0312)$ . With the exception of  $\Lambda_1$ , these values are taken from Zhou (2001) (who takes  $\Lambda_1 = 0$ ). They were estimated from weekly observations of the Federal Funds rate between 1954 and 1999.

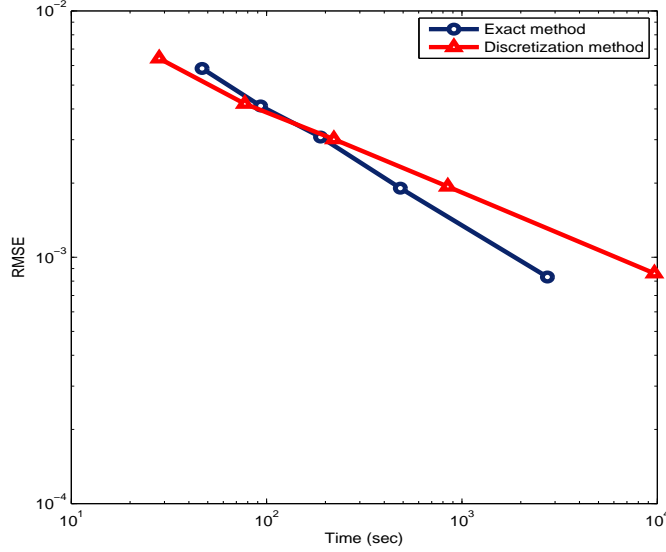


Figure 5: Convergence of the RMSEs for the Asian put in Table 2.

## 7.2 Exact method

For the specification (42), the Lamperti transform takes the form

$$F(x) = 2 \frac{\sqrt{x} - \sqrt{X_0}}{\sigma}. \quad (45)$$

It maps  $D_X = (0, \infty)$  into  $D_Y = (-2\sqrt{X_0}/\sigma, \infty)$ . The drift function (8) of the unit-volatility jump-diffusion  $Y = F(X)$  satisfying the SDE (7), is given by

$$\mu_Y(y) = \frac{4\kappa\theta - \sigma^2}{2\sigma^2(x + 2\sqrt{X_0}/\sigma)} - \frac{\kappa}{2} \left( x + 2\frac{\sqrt{X_0}}{\sigma} \right), \quad y \in (-2\sqrt{X_0}/\sigma, \infty). \quad (46)$$

The jump size function (10) of  $Y$  takes the form

$$\Delta_Y(y, z) = F(F^{-1}(y) + z) - y = 2 \frac{((\sqrt{X_0} + y\frac{\sigma}{2})^2 + z)^{1/2} - \sqrt{X_0}}{\sigma} - y. \quad (47)$$

The lower boundary of  $D_Y$  is unattainable due to the Feller property  $2\kappa\theta > \sigma^2$ . Also the boundary  $+\infty$  is unattainable.

Method	Trials	Steps	Value	Bias	SE	RMSE	Time (sec)
Exact	10K	N/A	1.2573	0	0.1430	0.1430	33.06
	20K	N/A	1.2783	0	0.1005	0.1005	68.24
	40K	N/A	1.2914	0	0.0717	0.0717	140.05
	100K	N/A	1.2597	0	0.0453	0.0453	383.67
	500K	N/A	1.2778	0	0.0202	0.0202	1681.31
Discretization	10K	100	1.3519	0.0221	0.1433	0.1450	26.50
	20K	140	1.2586	0.0144	0.1014	0.1024	75.20
	40K	200	1.2736	0.0094	0.0718	0.0724	220.73
	100K	310	1.2836	0.0058	0.0454	0.0458	836.57
	500K	707	1.2792	0.0013	0.0203	0.0203	9384.41

Table 3: Simulation results under the model (31) for a down-and-out call option with strike price  $K = 65$ , barrier  $B = 5$  and expiration date  $T = 1$  year. The parameter values are  $X_0 = 50$ ,  $\beta = -1$ ,  $r = 0.05$ ,  $a = 50/4$ ,  $b = 0$ , and  $c = 1/2$ . The true value is 1.2794.

### 7.3 Discretization method

The process  $X$  follows a Feller diffusion between two jump times. For time steps of length  $h = T/I$ , the discretization  $\widehat{X}$  of  $X$  between jump times is

$$\widehat{X}_{i+1} = \widehat{X}_i + \kappa(\theta - \widehat{X}_i^+) + \sigma(\widehat{X}_i^+)^{1/2}\mathcal{N}_i, \quad (48)$$

where  $x^+ = \max(0, x)$ . Lord, Koekkoek & Van Dijk (2010) find that, when used in the discretization of the Heston model, the scheme (48) produces the smallest discretization error among several alternative truncation and reflection schemes. They also prove strong convergence of this scheme. A disadvantage of (48) is that  $\widehat{X}_{i+1}$  may become negative with positive probability. We address this issue by taking  $\Lambda(x) = \Lambda_0 + \Lambda_1 x^+$  when evaluating the intensity on the discretization grid. An alternative first order scheme that guarantees positivity and also strongly converges is proposed by Alfonsi (2005):

$$\widehat{X}_{i+1} = \left\{ (1 - \kappa h/2)(\widehat{X}_i)^{1/2} + \frac{\sigma \mathcal{N}_i}{2(1 - \kappa h/2)} \right\}^2 + (\kappa\theta - \sigma^2/4)h. \quad (49)$$

This scheme is valid if  $\kappa h \neq 2$  and  $4\kappa\theta \geq \sigma^2$ . Also the second order scheme of Alfonsi (2010, Proposition 2.1) guarantees positivity. It is valid if  $4\kappa\theta \geq \sigma^2$ :

$$\begin{aligned} \widehat{X}_{i+1} = e^{-\kappa h/2} \left\{ \left( (\theta\kappa - \sigma^2/4) \frac{1 - e^{-\kappa h/2}}{\kappa} + e^{-\kappa h/2} \widehat{X}_i \right)^{1/2} + \frac{\sigma \mathcal{N}_i}{2} \right\}^2 \\ + (\kappa\theta - \sigma^2/4) \frac{1 - e^{-\kappa h/2}}{\kappa}. \end{aligned} \quad (50)$$

A time-scaling scheme similar to the one described in Section 5.3 above is used to

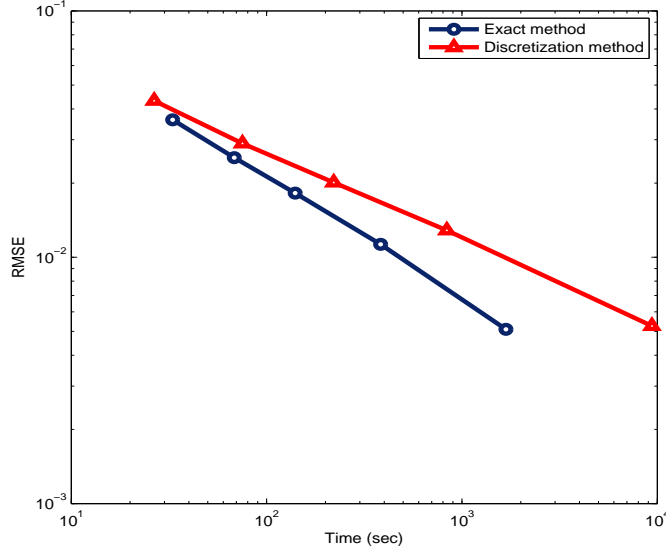


Figure 6: Convergence of the RMSEs for the down-and-out call in Table 3.

generate the jump times  $T_n$ .

## 7.4 Zero bond and cap

We estimate  $\mathbb{E}(\exp(-\int_0^T X_s ds))$ , the price of a zero-coupon bond with unit face value and maturity  $T = 3$  years, and  $\mathbb{E}(\sum_{t=1}^3 \exp(-\int_0^t X_s ds)(X_t - K)^+)$ , the price of a “cap” struck at  $K = 0.05$  with maturity  $T = 3$  years. We use the exact algorithm described in Section 4.3, the discretization scheme (48), denoted “Discretization I”, the scheme (49), denoted “Discretization II,” and the scheme (50), denoted “Discretization III.”<sup>1</sup> The discretization schemes approximate  $\int_0^T X_s ds$  using the trapezoidal rule. The number of discretization time steps is set equal to the square-root of the number of simulation trials.

Tables 4 and 5 report the results for the exact and discretization methods. The true values of the securities were computed using the transform results of Duffie et al. (2000). Figures 7 and 8 show the convergence of the RMSEs. The exact method achieves the optimal square-root convergence. The convergence rate of the discretization schemes is slower, indicating the significance of the bias. The second order method slightly outperforms the two first order methods.

<sup>1</sup>Because the intensity is unbounded, the model (42) falls outside the scope of the exact scheme of Casella & Roberts (2011). The exact scheme of Giesecke et al. (2010) produces exact samples of a skeleton of  $X$ ; these do, however, not suffice to obtain an unbiased estimator of the bond price.

Method	Trials	Steps	Value	Bias	SE	RMSE	Time (sec)
Exact	10K	N/A	0.880506	0	7.672E-04	7.672E-04	15.98
	20K	N/A	0.880233	0	5.381E-04	5.381E-04	31.42
	40K	N/A	0.880077	0	3.814E-04	3.814E-04	63.73
	100K	N/A	0.880239	0	2.430E-04	2.430E-04	170.06
	500K	N/A	0.879786	0	1.086E-04	1.086E-04	787.16
Discretization I	10K	100	0.878598	1.137E-03	1.011E-04	1.142E-03	30.06
	20K	140	0.879160	8.080E-04	6.845E-05	8.109E-04	83.65
	40K	200	0.879244	5.637E-04	4.924E-05	5.659E-04	235.91
	100K	310	0.879535	3.659E-04	3.103E-05	3.672E-04	920.84
	500K	707	0.879721	1.677E-04	1.393E-05	1.683E-04	10424.40
Discretization II	10K	100	0.878690	1.141E-03	9.952E-05	1.146E-03	30.65
	20K	140	0.879160	8.056E-04	6.954E-05	8.086E-04	82.24
	40K	200	0.879386	5.673E-04	4.924E-05	5.694E-04	234.27
	100K	310	0.879494	3.661E-04	3.111E-05	3.675E-04	912.30
	500K	707	0.879697	1.652E-04	1.396E-05	1.658E-04	10240.42
Discretization III	10K	100	0.878723	1.137E-03	9.881E-05	1.141E-03	29.16
	20K	140	0.879076	8.096E-04	7.052E-05	8.126E-04	82.27
	40K	200	0.879278	5.674E-04	4.996E-05	5.652E-04	237.06
	100K	310	0.879505	3.661E-04	3.121E-05	3.650E-04	916.99
	500K	707	0.879716	1.652E-04	1.391E-05	1.658E-04	9733.03

Table 4: Simulation results under the model (42) for a bond with maturity  $T = 3$  years. The parameter values are  $X_0 = \theta = 0.0422$ ,  $\kappa = 0.0117$ ,  $\sigma = 0.013$ ,  $\Lambda_0 = 0.011$ ,  $\Lambda_1 = 0.1$ ,  $\alpha = 0.0113$ ,  $\beta = 0.0312$ . The true value of the bond is 0.879872.

## 8 Conclusion

This paper develops and evaluates an acceptance/rejection algorithm for the exact sampling of a one-dimensional jump-diffusion with state-dependent drift, volatility, jump intensity, and jump size. The algorithm requires the drift function to be  $C^1$ , the volatility function to be  $C^2$ , and the jump intensity function to be locally bounded. It can be used to treat functionals depending on a skeleton of the jump-diffusion, the complete path of the jump component, a hitting time, the value of the jump-diffusion at the hitting time, and the exponential of the integrated jump-diffusion. The exact method leads to unbiased simulation estimators of security prices, transition densities, hitting probabilities and other quantities. Numerical results illustrate the behavior of the exact method.

## A Likelihood ratio formula

We provide a formula for the likelihood ratio required in the acceptance test described in Section 5.3. Recall that the transformed process  $Y$  solves the SDE (7), and that the

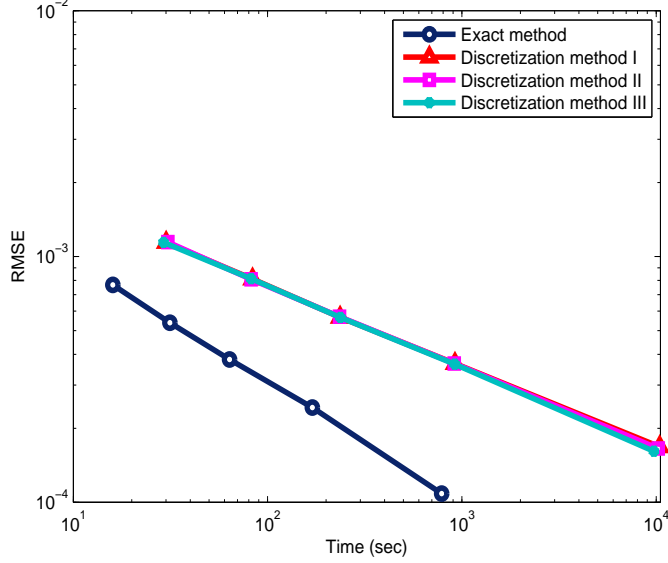


Figure 7: Convergence of the RMSEs for the bond in Table 4.

unit-diffusion  $\bar{Y}$  solves the SDE (17). Let  $(\bar{\mathcal{F}}_t)_{t \geq 0}$  be the filtration generated by  $\bar{Y}$ . For some  $s \geq 0$ , fixing  $Y_s = y$ , we are interested in sampling the values  $\bar{Y}_t$  from  $t = s$  up to the first exit time of  $\bar{Y}$  from the interval  $[y - \theta, y + \theta]$ , where  $\theta > 0$ .

Without loss of generality, we take  $D_Y = [y, \infty)$ . Fix  $\theta > 0$  such that  $-\theta > \underline{y}$ . Consider the exit time  $\zeta = \inf\{t \geq s : |\bar{Y}_t - y| \geq \theta\}$ . Let  $\bar{\mathbb{P}} = \bar{\mathbb{P}}_{(y;s,t)}$  be the  $\mathbb{P}$ -law on the  $\sigma$ -field  $\bar{\mathcal{F}}_{t \wedge \zeta}$  of the path  $\{\bar{Y}_{u \wedge \zeta}, s \leq u \leq t \wedge \zeta\}$ . We provide a formula for the likelihood ratio between  $\bar{\mathbb{P}}$  and an equivalent measure  $\mathbb{Q} = \mathbb{Q}_{(y;s,t)}$  on  $\bar{\mathcal{F}}_{t \wedge \zeta}$  under which  $\{\bar{Y}_{u \wedge \zeta}, s \leq u \leq t \wedge \zeta\}$  is a path of a standard Brownian motion stopped at  $\zeta$ .

**Proposition A.1.** *Suppose the jump-diffusion  $X$  satisfies Assumptions 2.1 and 2.2. Then for any event  $B \in \bar{\mathcal{F}}_{t \wedge \zeta}$  we have the formula*

$$\frac{\bar{\mathbb{P}}(B)}{\mathbb{Q}(B)} = \mathbb{E}^{\mathbb{Q}} \left[ \exp \left( A(y + W_{t \wedge \tau}^{\mathbb{Q}}) - A(y) - \int_s^{t \wedge \tau} \phi(y + W_u^{\mathbb{Q}}) du \right) \middle| B \right]$$

where  $W^{\mathbb{Q}}$  is a  $\mathbb{Q}$ -Brownian motion starting at  $W_s^{\mathbb{Q}} = 0$  and  $\tau = \inf\{t \geq 0 : |W_t| \geq \theta\}$ .

*Proof.* Consider the supermartingale  $Z = (Z_t)_{t \geq s}$  defined by

$$Z_t = \exp \left( - \int_s^{t \wedge \zeta} \mu_Y(\bar{Y}_u) dW_u - \frac{1}{2} \int_s^{t \wedge \zeta} \mu_Y^2(\bar{Y}_u) du \right). \quad (51)$$

From Assumption 2.1 it follows that  $\mu_Y$  is continuous on the interior of  $D_Y$ . Since by definition of  $\zeta$  and the choice of  $\theta$ ,  $\bar{Y}_u \in \text{Int } D_Y$  for all  $u \leq \zeta$ ,  $\mu_Y^2(\bar{Y}_u)$  is bounded from below and from above for  $u \leq \zeta$ , and so is  $\mu_Y(\bar{Y}_u)$ . If we define  $M_Y$  to be the max of

Method	Trials	Steps	Value	Bias	SE	RMSE	Time (sec)
Exact	10K	N/A	0.001202	0	6.225E-05	6.225E-05	16.17
	20K	N/A	0.001234	0	4.490E-05	4.490E-05	33.71
	40K	N/A	0.001257	0	3.170E-05	3.170E-05	64.02
	100K	N/A	0.001202	0	1.989E-05	1.989E-05	155.01
	500K	N/A	0.001203	0	8.844E-06	8.844E-06	773.53
Discretization I	10K	100	0.001171	2.301E-05	6.176E-05	6.591E-05	28.39
	20K	140	0.001134	1.223E-05	4.173E-05	4.349E-05	77.73
	40K	200	0.001234	7.181E-06	3.151E-05	3.231E-05	221.58
	100K	310	0.001201	5.544E-06	1.948E-05	2.025E-05	918.79
	500K	707	0.001205	4.765E-06	8.762E-06	9.974E-06	9690.47
Discretization II	10K	100	0.001221	2.121E-05	6.225E-05	6.577E-05	28.65
	20K	140	0.001207	1.452E-05	4.375E-05	4.610E-05	79.14
	40K	200	0.001139	1.151E-05	2.996E-05	3.209E-05	224.72
	100K	310	0.001229	7.445E-06	1.999E-05	2.133E-05	884.63
	500K	707	0.001217	7.473E-07	8.837E-06	8.869E-06	9823.68
Discretization III	10K	100	0.001198	2.335E-05	6.103E-05	6.534E-05	30.63
	20K	140	0.001180	7.036E-06	4.258E-05	4.316E-05	85.04
	40K	200	0.001179	6.606E-06	3.055E-05	3.126E-05	243.78
	100K	310	0.001196	6.437E-06	1.955E-05	2.059E-05	968.95
	500K	707	0.001197	2.045E-07	8.744E-06	8.746E-06	9893.69

Table 5: Simulation results under the model (42) for a cap with maturity  $T = 3$  years, strike  $K = 0.05$  and annual payments. The parameter values are  $X_0 = \theta = 0.0422$ ,  $\kappa = 0.0117$ ,  $\sigma = 0.013$ ,  $\Lambda_0 = 0.011$ ,  $\Lambda_1 = 0.1$ ,  $\alpha = 0.0113$ ,  $\beta = 0.0312$ . The true value of the cap is 0.001196.

$|\mu_Y(z)|$  over  $z \in [y - \theta, y + \theta]$ , then

$$\mathbb{E} \left[ \exp \left( \frac{1}{2} \int_0^t \mu_Y^2(\bar{Y}_{u \wedge \zeta}) du \right) \right] < \exp \left( \frac{1}{2} M_Y^2 t \right) < \infty$$

for any  $t$ . Thus Novikov's condition holds, guaranteeing that  $Z$  is a martingale. Moreover, since  $\mu_Y(\bar{Y}_{u \wedge \zeta}) \leq M_Y < \infty$  almost surely,  $Z_t > 0$  almost surely, so the process  $1/Z$  is well-defined.

Take  $d\mathbb{Q} = Z_t d\bar{\mathbb{P}}$ . By Girsanov's theorem, under  $\mathbb{Q}$ , the process

$$\bar{W}_{t \wedge \bar{\tau}}^{\mathbb{Q}} = W_{t \wedge \zeta} + \int_s^{t \wedge \zeta} \mu_Y(\bar{Y}_u) du = \bar{Y}_{t \wedge \zeta}, \quad t \geq s$$

is a standard Brownian motion started at  $\bar{W}_s^{\mathbb{Q}} = Y_s = y$  and stopped at time  $\bar{\tau} = \inf\{t \geq$

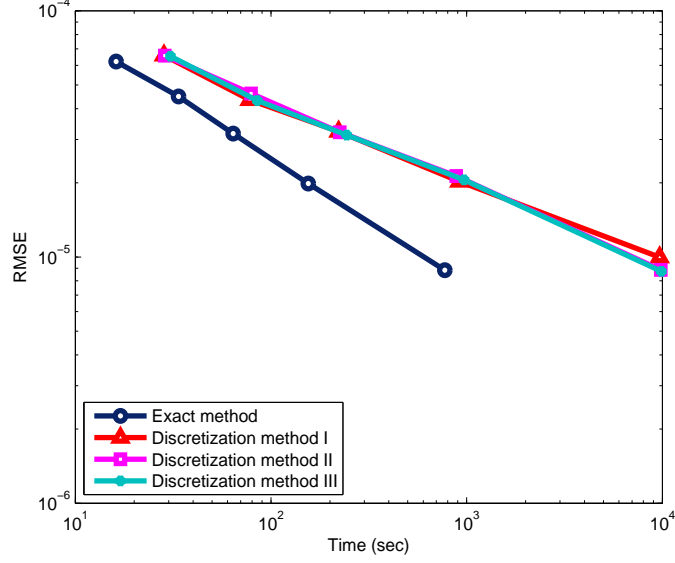


Figure 8: Convergence of the RMSEs for the cap in Table 5.

$s : |\bar{W}_t^{\mathbb{Q}} - y| \geq \theta\} = \zeta$ . Thus

$$\begin{aligned}
\frac{1}{Z_t} &= \exp\left(\int_s^{t \wedge \zeta} \mu_Y(\bar{Y}_u)(d\bar{Y}_u - \mu_Y(\bar{Y}_u)du) + \frac{1}{2} \int_s^{t \wedge \zeta} \mu_Y^2(\bar{Y}_u)du\right) \\
&= \exp\left(\int_s^{t \wedge \zeta} \mu_Y(\bar{Y}_u)d\bar{Y}_u - \frac{1}{2} \int_s^{t \wedge \zeta} \mu_Y^2(\bar{Y}_u)du\right) \\
&= \exp\left(\int_s^{t \wedge \bar{\tau}} \mu_Y(\bar{W}_u^{\mathbb{Q}})d\bar{W}_u^{\mathbb{Q}} - \frac{1}{2} \int_s^{t \wedge \bar{\tau}} \mu_Y^2(\bar{W}_u^{\mathbb{Q}})du\right).
\end{aligned}$$

Applying Itô's formula to  $1/Z$  we obtain

$$A(\bar{W}_{t \wedge \bar{\tau}}^{\mathbb{Q}}) = A(\bar{W}_0^{\mathbb{Q}}) + \int_0^{t \wedge \bar{\tau}} \mu_Y(\bar{W}_u^{\mathbb{Q}})d\bar{W}_u^{\mathbb{Q}} + \frac{1}{2} \int_0^{t \wedge \bar{\tau}} \mu_Y'(\bar{W}_u^{\mathbb{Q}})du$$

so that, for  $\phi = (\mu_Y^2 + \mu_Y')/2$ ,

$$\frac{1}{Z_t} = \exp\left(A(\bar{W}_{t \wedge \bar{\tau}}^{\mathbb{Q}}) - A(\bar{W}_0^{\mathbb{Q}}) - \int_0^{t \wedge \bar{\tau}} \phi(\bar{W}_u^{\mathbb{Q}})du\right).$$

By the translation property,  $W_t^{\mathbb{Q}} = \bar{W}_t^{\mathbb{Q}} - y$  is a  $\mathbb{Q}$ -Brownian motion starting at  $W_s^{\mathbb{Q}} = 0$ . Moreover,  $\tau = \inf\{t \geq s : |W_t| \geq \theta\} = \bar{\tau}$  almost surely. Thus

$$\frac{d\bar{\mathbb{P}}}{d\mathbb{Q}} = \frac{1}{Z_t} = \exp\left(A(y + W_{t \wedge \tau}^{\mathbb{Q}}) - A(y) - \int_s^{t \wedge \tau} \phi(y + W_u^{\mathbb{Q}})du\right).$$

Finally, for any set  $B \in \bar{\mathcal{F}}_{t \wedge \zeta}$ , we get

$$\begin{aligned} \bar{\mathbb{P}}(B) &= \mathbb{E}^{\mathbb{Q}}(1_B 1/Z_t) \\ &= \mathbb{E}^{\mathbb{Q}}(1/Z_t | B) \mathbb{Q}(B) \\ &= \mathbb{E}^{\mathbb{Q}} \left[ \exp \left( A(y + W_{t \wedge \tau}^{\mathbb{Q}}) - A(y) - \int_s^{t \wedge \tau} \phi(y + W_u^{\mathbb{Q}}) du \right) \middle| B \right] \mathbb{Q}(B) \end{aligned}$$

This proves the likelihood ratio formula. □

## References

- Ait-Sahalia, Yacine, Jianqing Fan & Heng Peng (2009), ‘Nonparametric transition-based tests for jump-diffusions’, *Journal of the American Statistical Association* **104**, 1102–1116.
- Alfonsi, Aurelien (2005), ‘On the discretization schemes for the CIR (and Bessel squared) processes’, *Monte Carlo Methods and Applications* **11**(4), 355–384.
- Alfonsi, Aurelien (2010), ‘High order discretization schemes for the CIR process: Application to affine term structure and Heston models’, *Mathematics of Computation* **79**(269), 209–237.
- Andersen, Leif & Dan Buffum (2003), ‘Calibration and implementation of convertible bond models’, *Journal of Computational Finance* **7**, 1–34.
- Arnsdorf, Matthias & Igor Halperin (2008), ‘BSLP: Markovian bivariate spread-loss model for portfolio credit derivatives’, *Journal of Computational Finance* **12**, 77–100.
- Ayache, E., Peter Forsyth & Kenneth Vetzal (2003), ‘The valuation of convertible bonds with credit risk’, *Journal of Derivatives* **9**, 11–29.
- Bandi, Federico & Thong Nguyen (2003), ‘On the functional estimation of jump-diffusion models’, *Journal of Econometrics* **116**, 293–328.
- Beskos, Alexander & Gareth Roberts (2005), ‘Exact simulation of diffusions’, *Annals of Applied Probability* **15**(4), 2422–2444.
- Broadie, Mark & Ozgur Kaya (2006), ‘Exact simulation of stochastic volatility and other affine jump diffusion processes’, *Operations Research* **54**(2), 217–231.
- Burq, Zaeem & Owen Jones (2008), ‘Simulation of Brownian motion at first-passage times’, *Mathematics and Computers in Simulation* **77**, 64–81.

- Carr, Peter & Dilip Madan (2010), ‘Local volatility enhanced by a jump to default’, *SIAM Journal on Financial Mathematics* **1**, 2–15.
- Carr, Peter & Vadim Linetsky (2006), ‘A jump to default extended CEV model: an application of Bessel processes’, *Finance and Stochastics* **10**, 303–330.
- Casella, Bruno & Gareth Roberts (2011), ‘Exact simulation of jump-diffusion processes with Monte Carlo applications’, *Methodology and Computing in Applied Probability* **13**(3), 449–473.
- Chen, Nan (2009), Localization and exact simulation of Brownian motion driven stochastic differential equations. Working Paper, Chinese University of Hong Kong.
- Davis, Mark & Fabian Lischka (2002), Convertible bonds with market and credit risk, in R.Chan, Y.-K.Kwok, D.Yao & Q.Zhang, eds, ‘Applied Probability’, Studies in Advanced Mathematics, American Mathematical Society/International Press, pp. 45–58.
- Ding, Xiaowei, Kay Giesecke & Pascal Tomecek (2009), ‘Time-changed birth processes and multi-name credit derivatives’, *Operations Research* **57**(4), 990–1005.
- Duffie, Darrell, Jun Pan & Kenneth Singleton (2000), ‘Transform analysis and asset pricing for affine jump-diffusions’, *Econometrica* **68**, 1343–1376.
- Duffie, Darrell & Kenneth J. Singleton (1999), ‘Modeling term structures of defaultable bonds’, *Review of Financial Studies* **12**, 687–720.
- Duffie, Darrell & Peter Glynn (1995), ‘Efficient Monte Carlo estimation of security prices’, *Annals of Applied Probability* **4**(5), 897–905.
- Errais, Eymen, Kay Giesecke & Lisa Goldberg (2010), ‘Affine point processes and portfolio credit risk’, *SIAM Journal on Financial Mathematics* **1**, 642–665.
- Giesecke, Kay, Hossein Kakavand & Mohammad Mousavi (2010), Exact simulation of point processes with stochastic intensities. *Operations Research*, forthcoming.
- Glasserman, Paul & Nicolas Merener (2003), ‘Numerical solution of jump-diffusion LIBOR market models’, *Finance and Stochastics* **7**, 1–27.
- Ikeda, Nobuyuki & Shinzo Watanabe (1989), *Stochastic differential equations and diffusion processes*, North Holland, New York.
- Imhof, Peter (1984), ‘Density factorizations for Brownian motion, meander and the three-dimensional Bessel process’, *Journal of Applied Probability* **21**, 500–510.
- Johannes, Michael (2004), ‘The statistical and economic role of jumps in continuous-time interest rate models’, *Journal of Finance* **59**, 227–260.

- Kou, Steve (2002), ‘A jump-diffusion model for option pricing’, *Management Science* **48**, 1086–1101.
- Kou, Steve & Hui Wang (2004), ‘Option pricing under a double exponential jump-diffusion model’, *Management Science* **50**, 1178–1192.
- Linetsky, Vadim (2006), ‘Pricing equity derivatives subject to bankruptcy’, *Mathematical Finance* **16**, 255–282.
- Lord, Roger, Remmert Koekkoek & Dick Van Dijk (2010), ‘A comparison of biased simulation schemes for stochastic volatility models’, *Quantitative Finance* **10**(2), 177–194.
- Madan, Dilip B. & Haluk Unal (1998), ‘Pricing the risks of default’, *Review of Derivatives Research* **2**, 121–160.
- Mendoza, Rafael, Peter Carr & Vadim Linetsky (2010), ‘Time-changed markov processes in unified credit-equity modeling’, *Mathematical Finance* **20**(4), 527–569.
- Merton, Robert C. (1976), ‘Option pricing when the underlying stock returns are discontinuous’, *Journal of Financial Economics* **3**, 123–144.
- Meyer, Paul-André (1971), Démonstration simplifiée d’un théorème de Knight, in ‘Séminaire de Probabilités V, Lecture Notes in Mathematics 191’, Springer-Verlag Berlin, pp. 191–195.
- Platen, Eckhard & Nicola Bruti-Liberati (2010), *Numerical Solution of Stochastic Differential Equations With Jumps in Finance*, Springer-Verlag, Berlin.
- Ruf, Johannes & Matthias Scherer (2011), ‘Pricing corporate bonds in an arbitrary jump-diffusion model based on an improved Brownian bridge algorithm’, *Journal of Computational Finance* **14**(3), 30–45.
- Williams, David (1970), ‘Decomposing the Brownian path’, *Bulletin of the American Mathematical Society* **76**, 871–873.
- Zhou, Chunsheng (2001), ‘The term structure of credit spreads with jump risk’, *Journal of Banking and Finance* **25**, 2015–2040.
- Zhou, Hao (2001), Jump-diffusion term structure and Ito conditional moment generator. Working Paper, Federal Reserve Board.